The significance of the defocus ATF

mild defocus $\quad \exp\left\{ i\pi \frac{x^2}{\lambda\delta} \right\} \approx 1 \quad \text{if} \quad \frac{(x'')_{\max}}{\lambda f_1} = \frac{(\mathrm{NA})}{\lambda} \ll \frac{1}{\sqrt{2\lambda\delta}} \Leftrightarrow \quad \delta \ll \frac{\lambda}{2\,(\mathrm{NA})^2}$

$$(\mathrm{DoF}) \equiv \frac{\lambda}{2\,(\mathrm{NA})^2}$$

Depth of Field

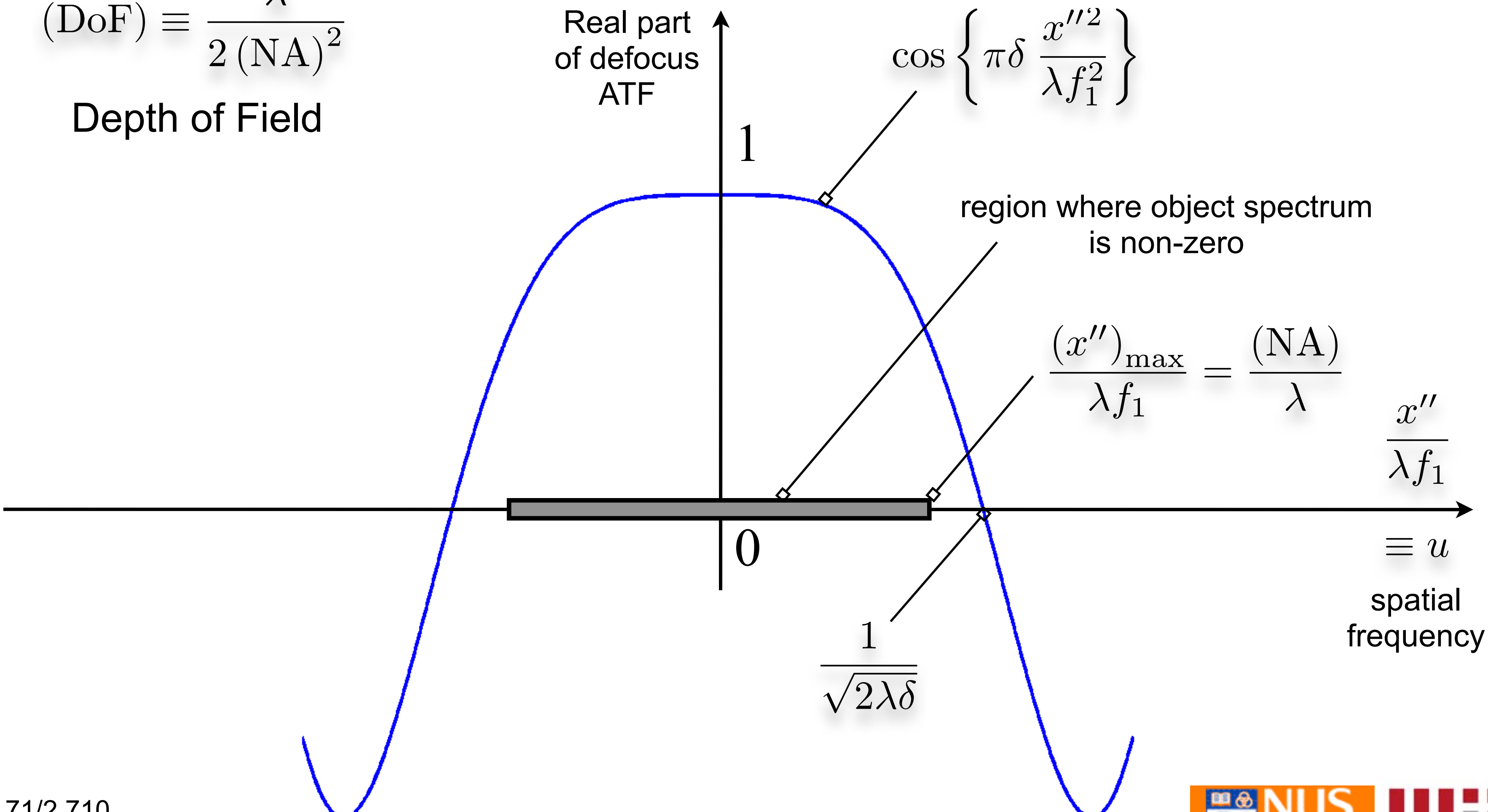

The significance of the defocus ATF

strong defocus $\delta > \dfrac{\lambda}{2\,(\mathrm{NA})^2}$

the oscillatory nature of the defocus kernel when $\delta>\mathrm{DoF}$ results in strong blur on the image because of the suppression of spatial frequencies near the nulls and sign changes at the negative portions

$$(\mathrm{DoF}) \equiv \frac{\lambda}{2\,(\mathrm{NA})^2}$$

Depth of Field

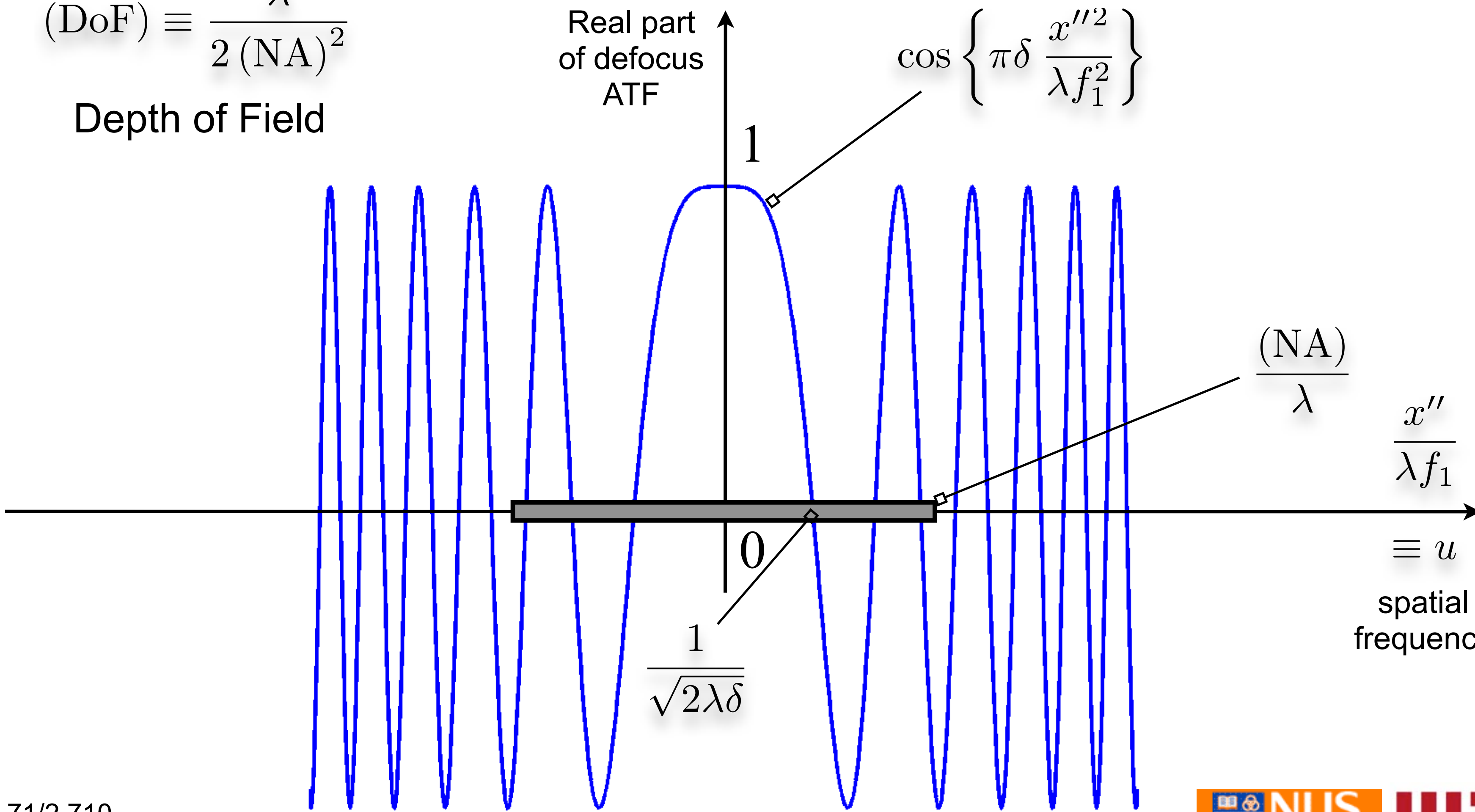

The significance of DoF in imaging

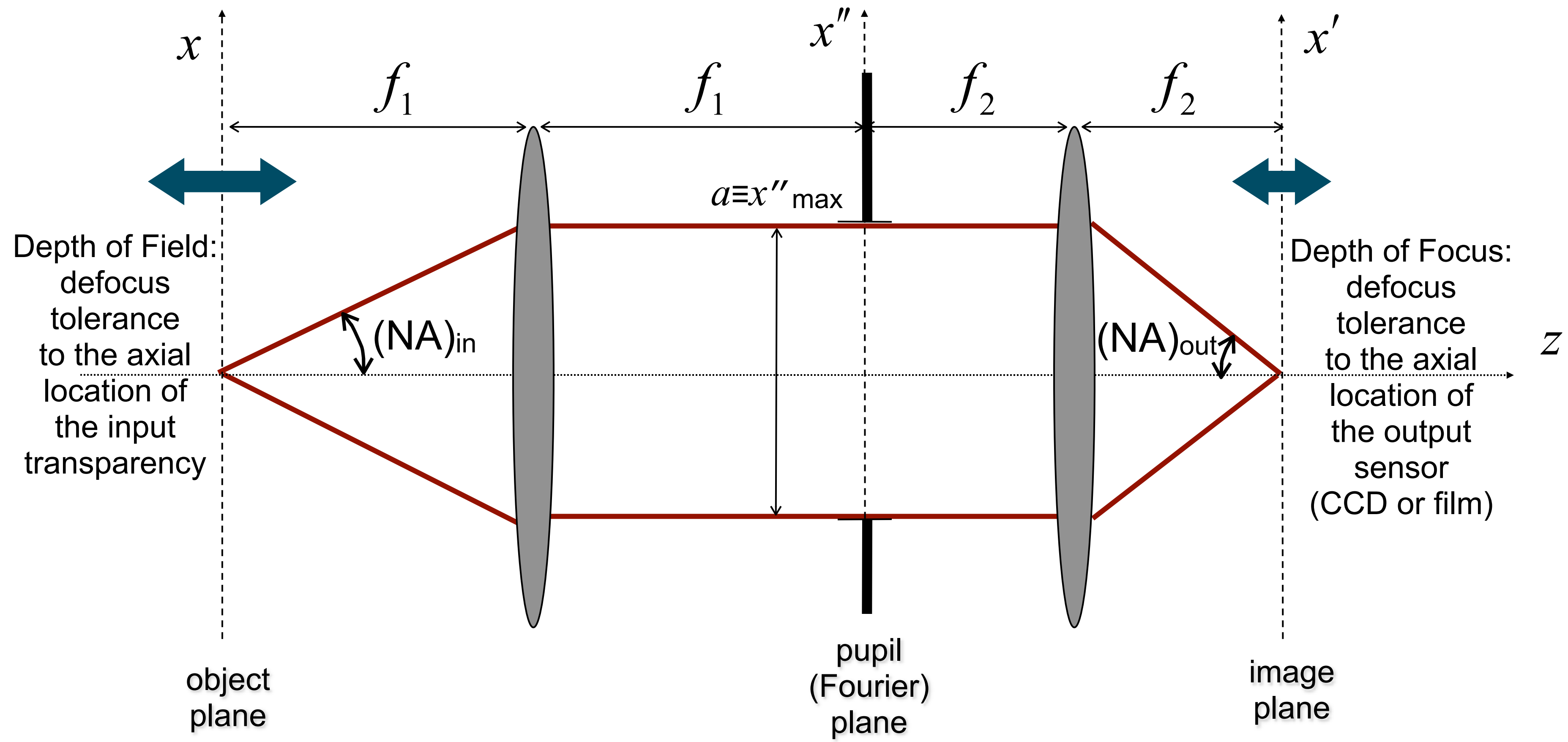

Numerical Aperture (in) $\quad (\mathrm{NA})_{\mathrm{in}} = \dfrac{(x'')_{\mathrm{max}}}{f_1}$ $\qquad$ Numerical Aperture (out) $\quad (\mathrm{NA})_{\mathrm{out}} = \dfrac{(x'')_{\mathrm{max}}}{f_2}$

Depth of Field $\quad (\mathrm{DoF}) = \dfrac{\lambda}{2\,(\mathrm{NA})_{\mathrm{in}}^2}$ $\qquad$ Depth of Focus $\quad (\mathrm{DoF}) = \dfrac{\lambda}{2\,(\mathrm{NA})_{\mathrm{out}}^2}$

Even though our derivations were carried out for *spatially coherent* imaging, the same arguments and results apply to the (more common) *spatially incoherent* case

The significance of DoF in imaging

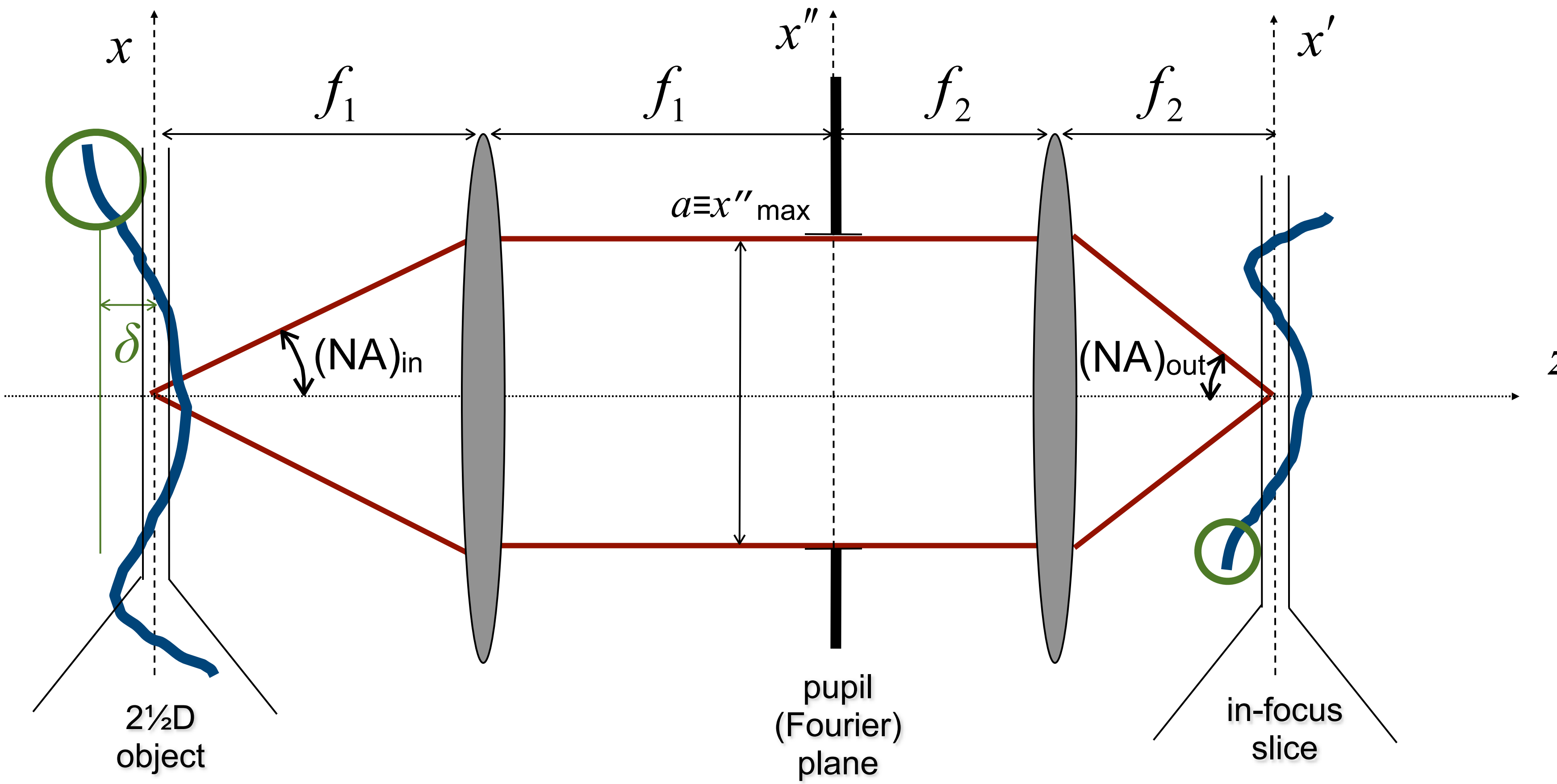

A portion of the object at distance δ from the focal plane is *locally* convolved with the defocus kernel $\exp\left\{i\pi \frac{x^2}{\lambda\delta}\right\}$

The point-spread function (PSF) now becomes a function of $\delta(x)$; therefore, the imaging system is now *shift variant*.

The portion within the in-focus axially cut slice $(\text{DoF}) = \frac{\lambda}{2\,(\text{NA})_{\text{in}}^2}$ is imaged with maximum sharpness on a slice of thickness $(\text{DoF}) = \frac{\lambda}{2\,(\text{NA})_{\text{out}}^2}$

Numerical examples: the object

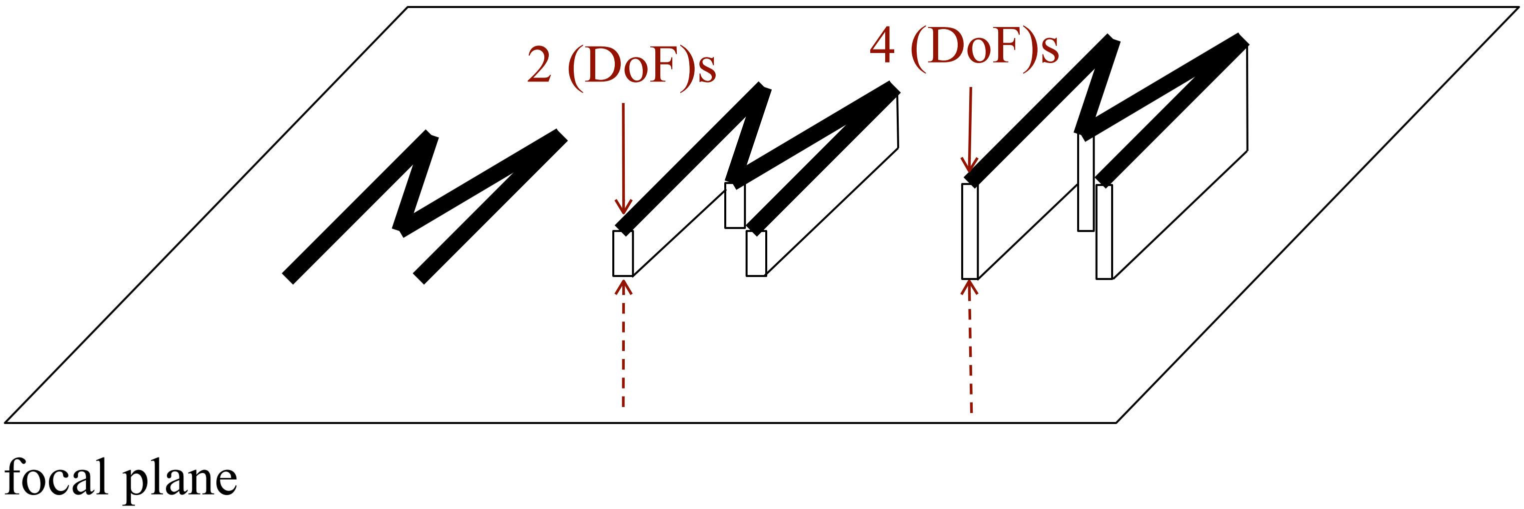

Intensity image: noise-free

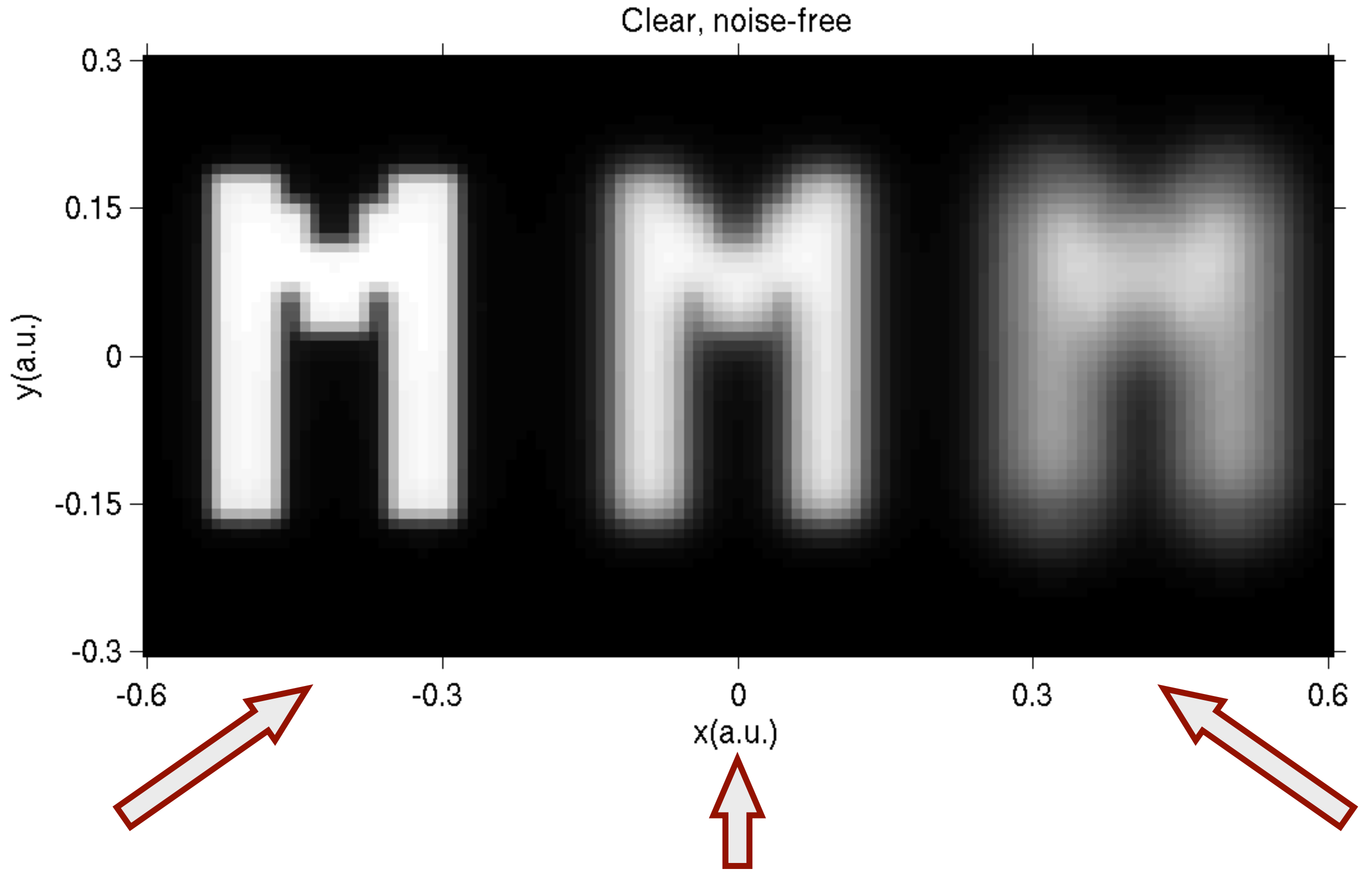

"M" convolved with standard diffraction-limited PSF

"M" convolved with diffraction-limited PSF *and* defocus equivalent to 2 DoFs

"M" convolved with diffraction-limited PSF *and* defocus equivalent to 4 DoFs

Can the blur be undone computationally?

- The effect of the optical system is expressed in the Fourier domain as a product of the object spectrum times the ATF:

$$G_{\mathrm{I}}^{\mathrm{out}}(u,v) = G_{\mathrm{I}}^{\mathrm{in}}(u,v) \times \boxed{\mathcal{H}(u,v)}$$

at best, diffraction-limited ATF; it may also include the effect of defocus and higher-order aberrations

- Therefore, if we multiply the image spectrum by the inverse ATF, we should expect to recover the original object:

$$G_{\mathrm{I}}^{\mathrm{in,recovered}}(u,v) = G_{\mathrm{I}}^{\mathrm{out}}(u,v) \times \frac{1}{\mathcal{H}(u,v)}$$

this is referred to as “inverse filtering” or “deconvolution”

- However, direct inversion *never* works because:
  - the ATF may be zero at certain locations, whence the inverse filter would blow up
  - the image intensity measurement always includes noise; the inverse filter typically amplifies the noise more than the true signal, leading to nasty artifacts in the reconstruction

Tikhonov-regularized inverse filter

- The following inverse filter behaves better than the direct inversion:

$$G_{\mathrm{I}}^{\mathrm{in,Tikhonov}}(u,v) = G_{\mathrm{I}}^{\mathrm{out}}(u,v) \times \frac{\mathcal{H}^*(u,v)}{|\mathcal{H}(u,v)|^2 + \mu}$$

  - for μ=0, it reduces to the direct filter (not a good idea)
  - the value of μ should be monotonically increasing with the amount of noise present in the intensity measurement
    - e.g. if the noise is vanishingly small then we expect direct inversion to be less problematic so a small value of μ is ok; however, the problem of zeros in the ATF remains so $\mu \neq 0$ is still necessary
    - if the noise is strong, then a large value of μ should be chosen to mitigate noise amplification at high frequencies
    - in the special case when both signal and noise obey Gaussian statistics, it can be shown that the optimal value of μ (in the sense of minimum quadratic error) is 1/SNR; this special case of a Tikhonov regularizer is also known as a **Wiener filter**

Tikhonov regularized inverse filter, noise-free

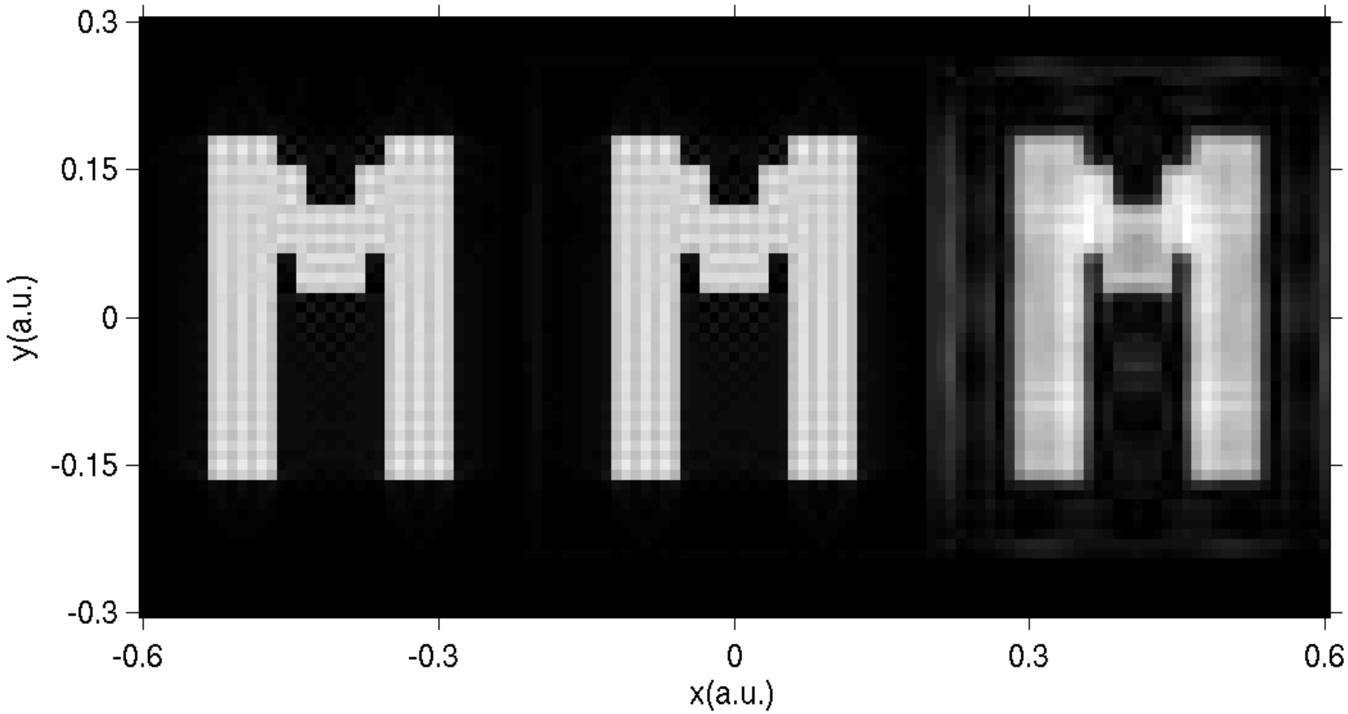

Deconvolution using Tikhonov regularized inverse filter
Utilized *a priori* knowledge of depth of each digit (alternatively, needs depth-from defocus algorithm)

Artifacts due primarily to numerical errors getting amplified by the inverse filter (despite regularization)

Intensity image: noisy

SNR=10

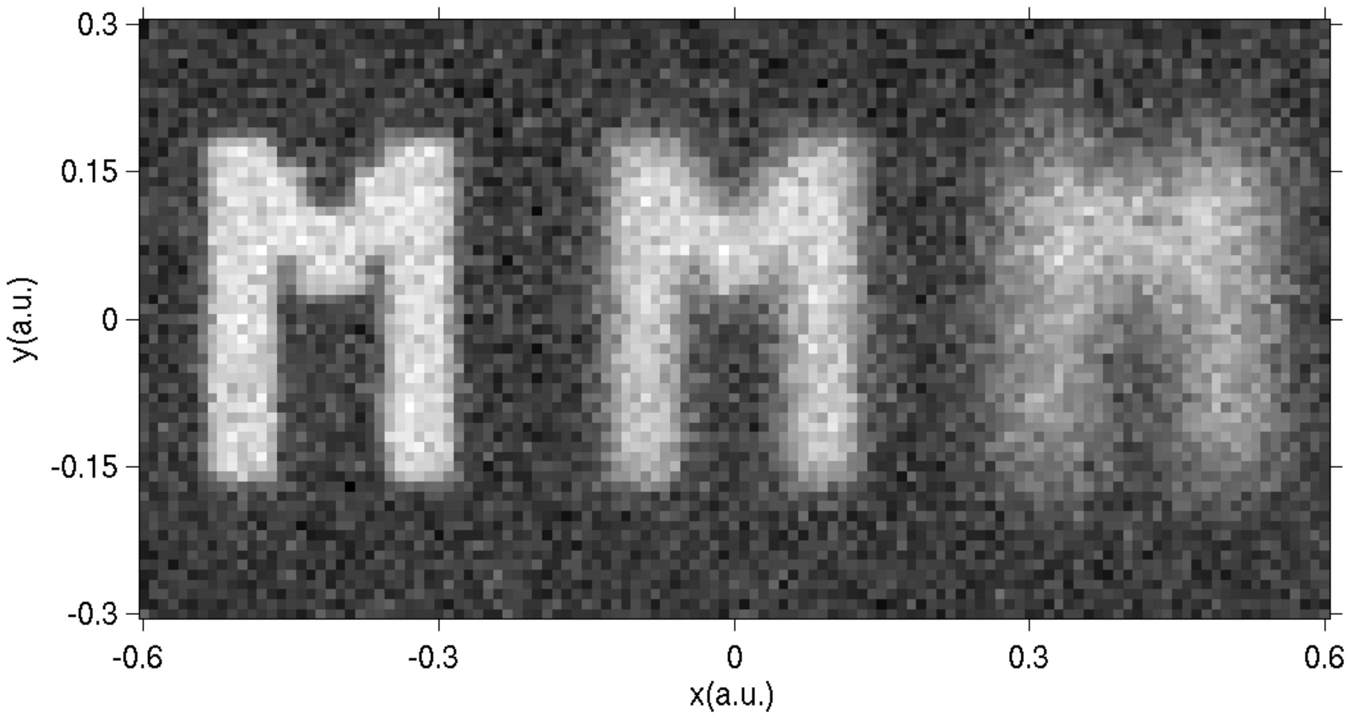

Tikhonov-regularized inverse filter with noise

SNR=10

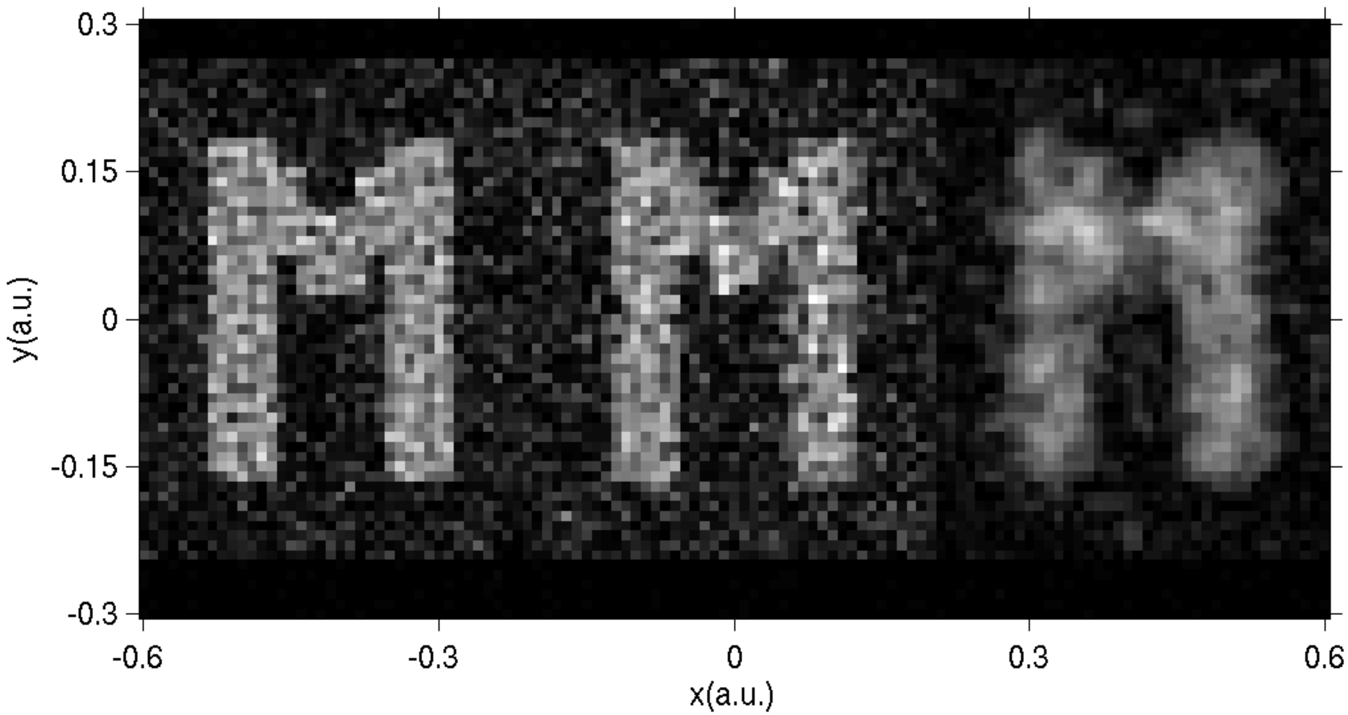

Deconvolution using Wiener filter (i.e. Tikhonov with μ=1/SNR=0.1)
Noise is destructive away from focus (especially at 4DOFs)
Utilized *a priori* knowledge of depth of each digit

Artifacts due primarily to noise getting amplified by the inverse filter

Today

- Polarization
  - the vector nature of electromagnetic waves revisited
  - basic polarizations: linear, circular
  - wave plates
  - polarization and interference
- Effects of polarization on imaging
  - beyond scalar optics: high Numerical Aperture
  - engineering the focal spot with special polarization modes

Vector nature of EM fields

Recall the vectorial nature of the EM wave equation: $$\nabla^2\mathbf{E} - \mu_o\epsilon_0 \frac{\partial^2 \mathbf{E}}{\partial t^2} = 0.$$

The polarization is given by the constitutive relationship: $$\mathbf{P} = f(\mathbf{E})$$

linear, isotropic $\mathbf{P} = \chi\mathbf{E}$

index of refraction

$$n = \sqrt{1+\chi}$$

linear, anisotropic $$\mathbf{P} = \begin{pmatrix} \chi_{11} & \chi_{12} & \chi_{13} \\ \chi_{21} & \chi_{22} & \chi_{23} \\ \chi_{31} & \chi_{32} & \chi_{33} \end{pmatrix} \mathbf{E}$$

The index of refraction (phase delay) depends on the polarization

non-linear, isotropic $\mathbf{P} = \chi_1\mathbf{E} + \chi_3 |\mathbf{E}|^2 \mathbf{E}$

χ_3 : Kerr coefficient

The index of refraction (phase delay) depends on the intensity

Linear polarization

Fixed time
("snapshot")

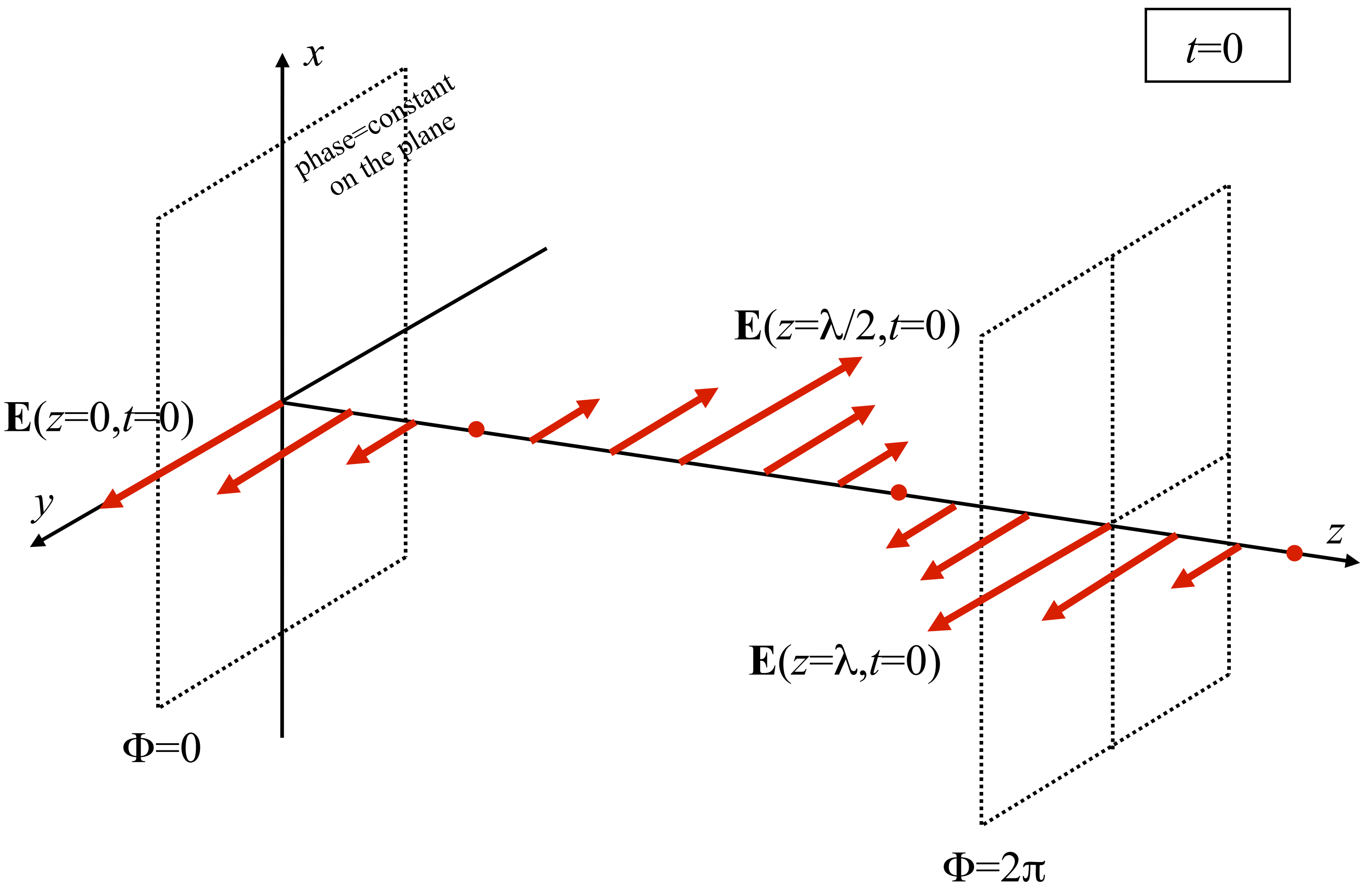

Linear polarization

Fixed space
("oscilloscope")

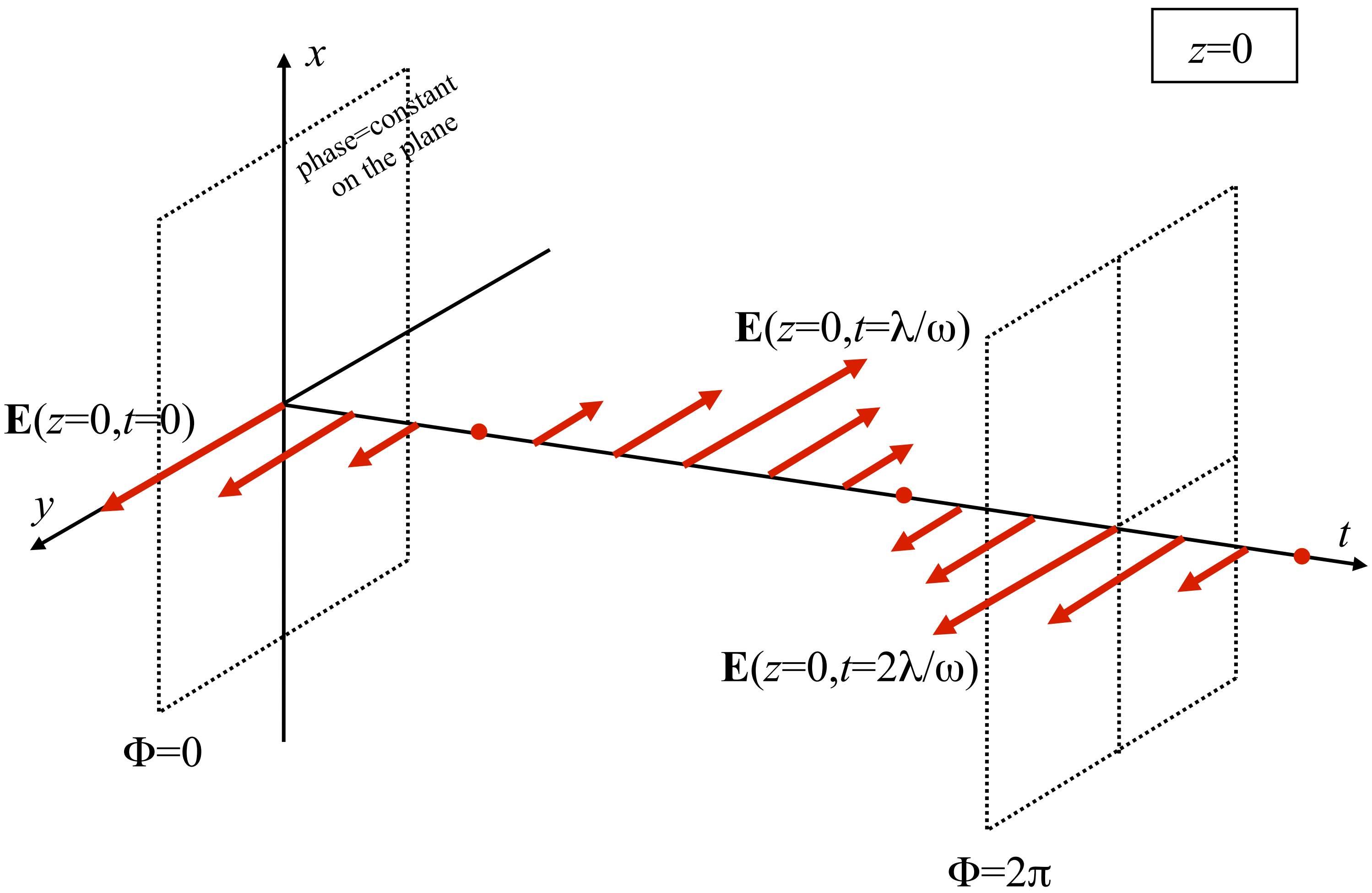

Circular polarization

Fixed time
("snapshot")

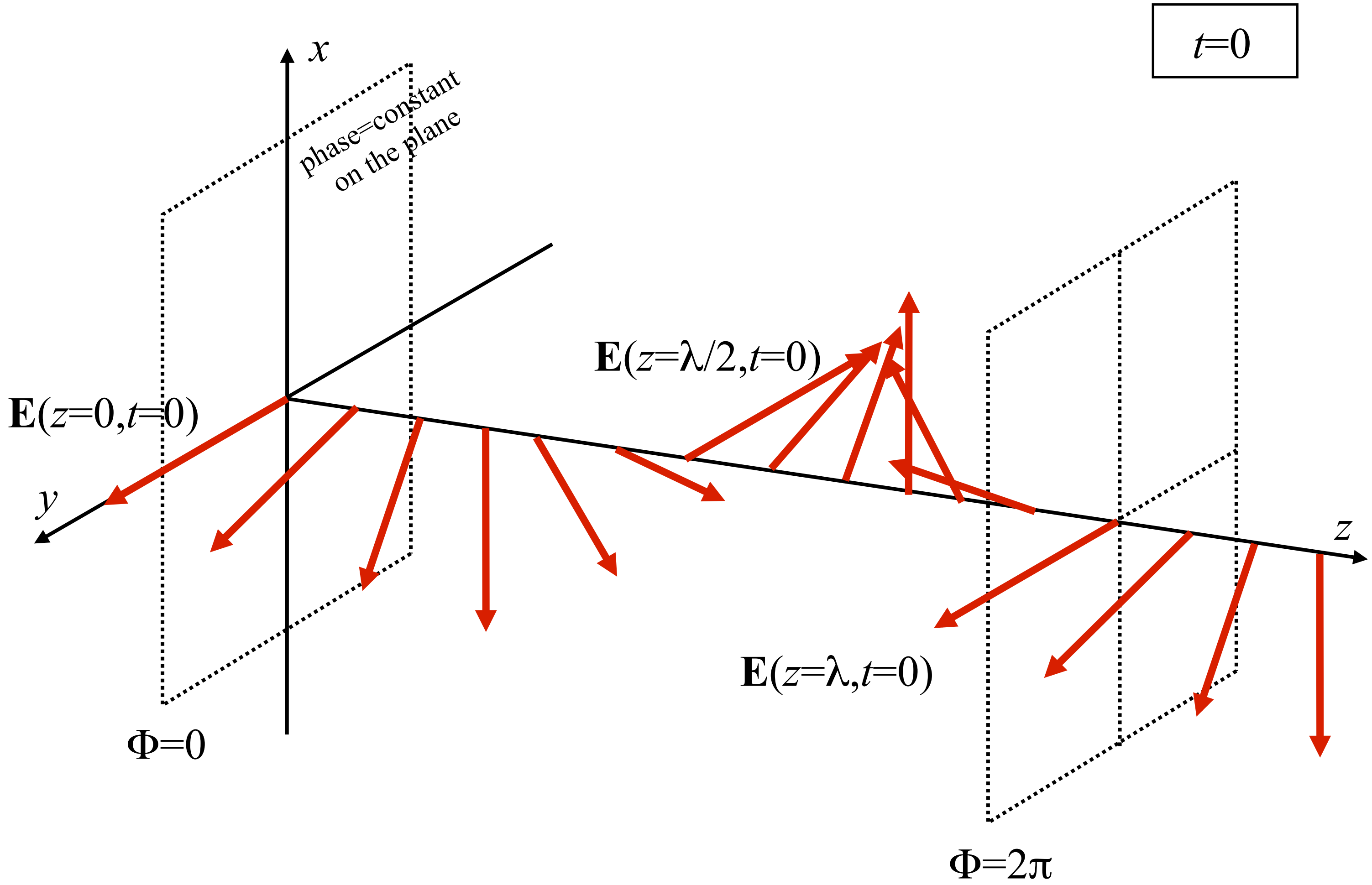

Circular polarization

Decomposition into the two basic linear polarizations
with $\pi/2$ phase delay

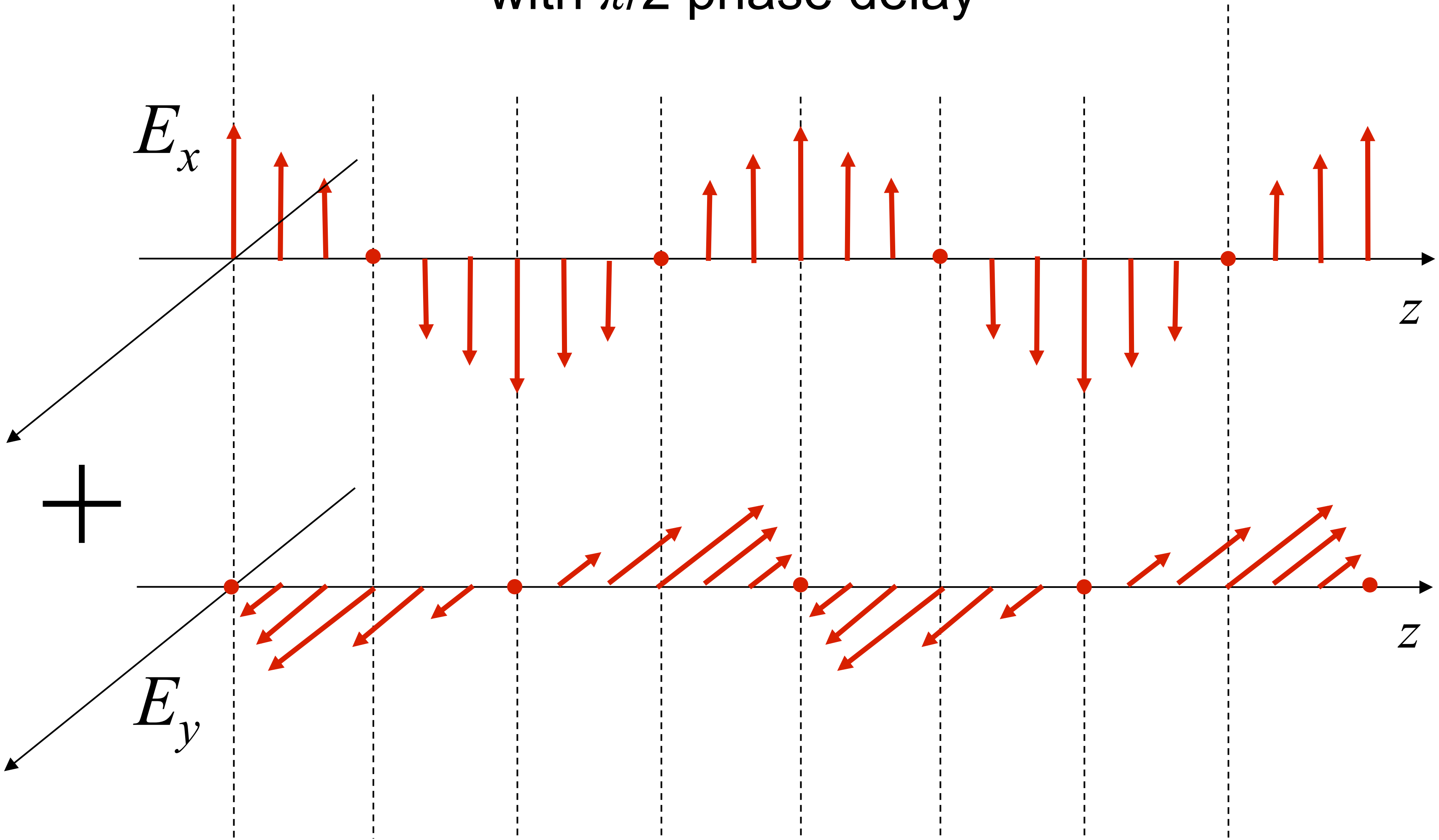

Circular polarization

Fixed space
("oscilloscope")

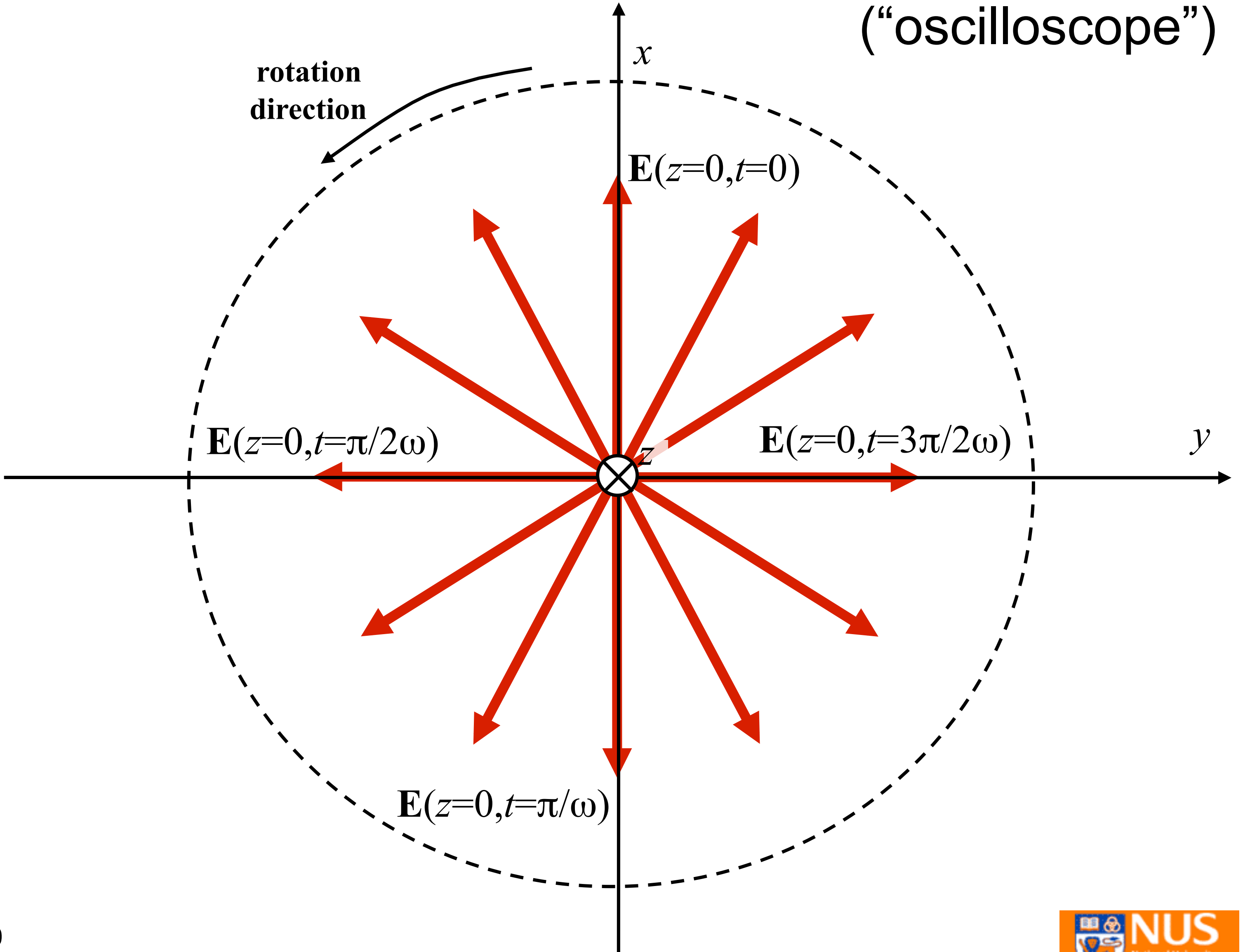

λ/4 wave plate

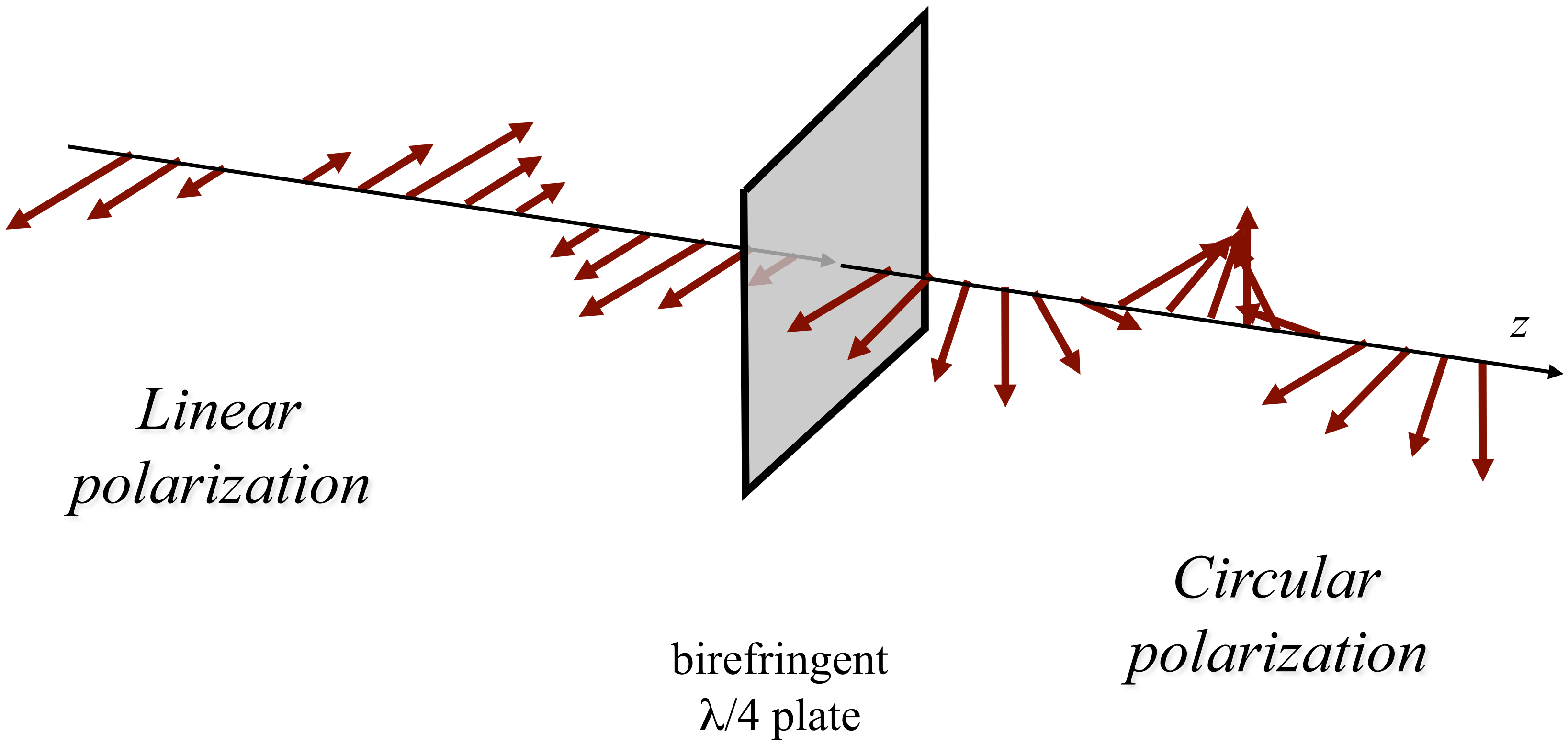

λ/2 wave plate

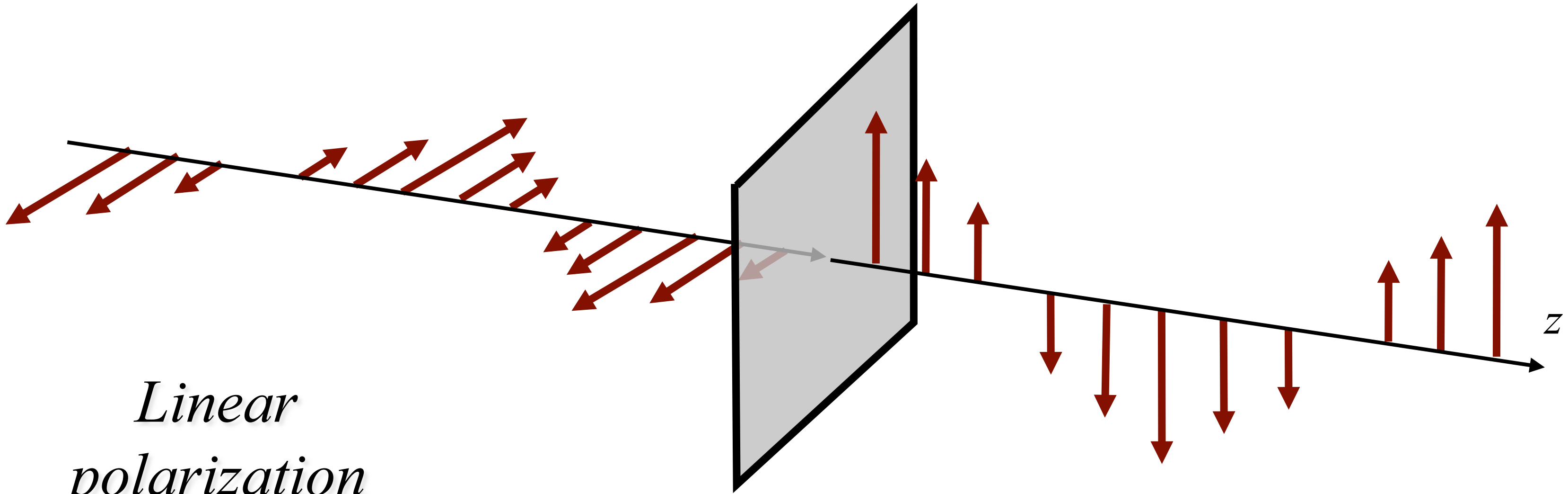

Think about that

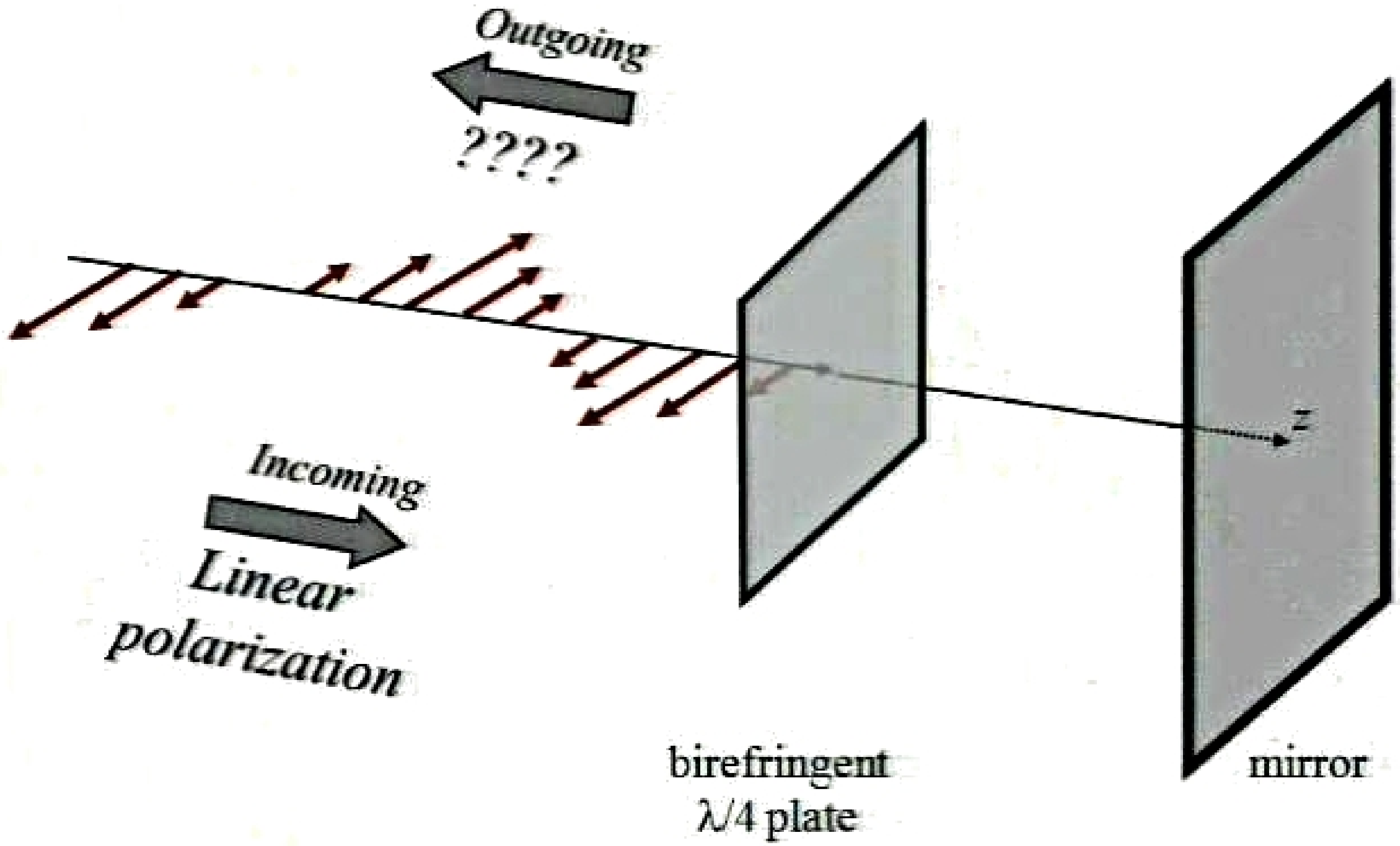

Polarization and interference

$$I = |\mathbf{E}_1 + \mathbf{E}_2|^2$$

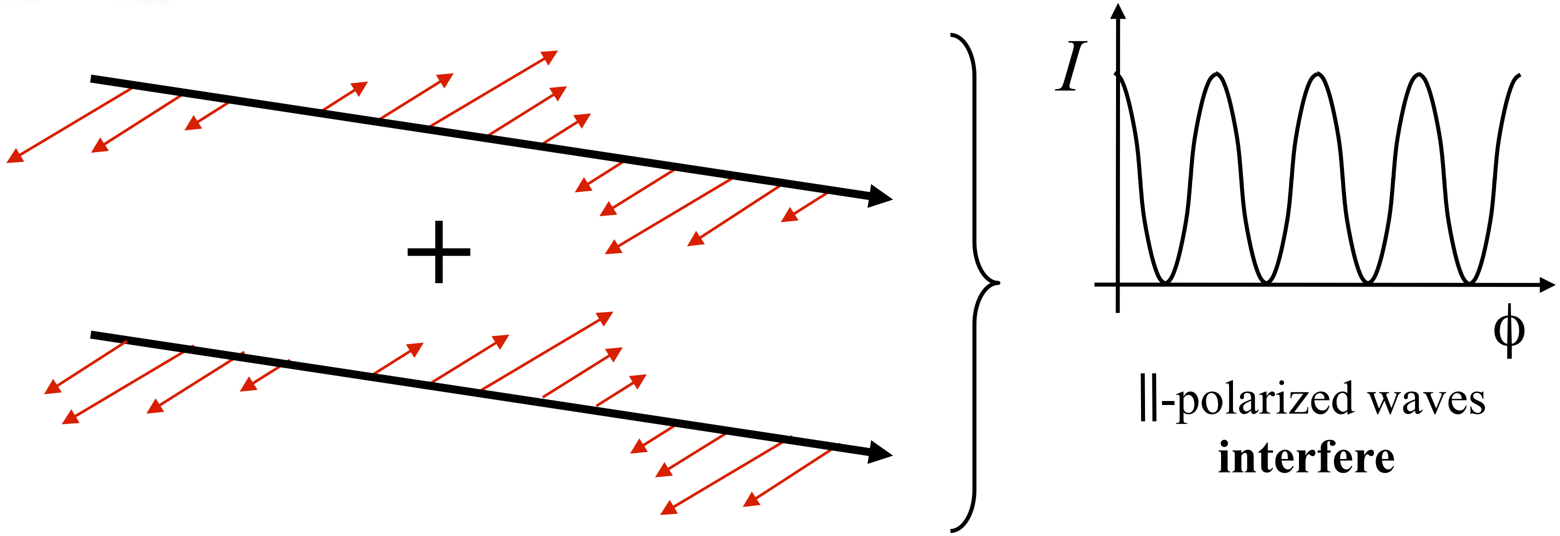

||-polarized waves
interfere

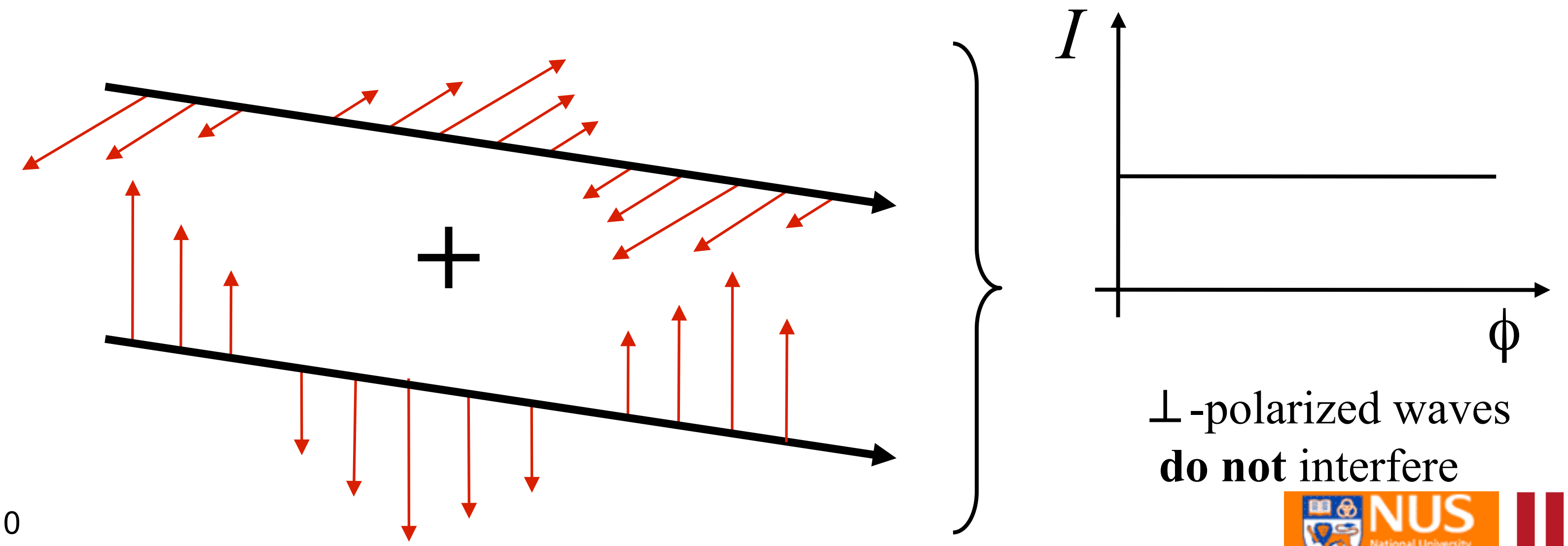

⊥-polarized waves
do not interfere

Intensity in focal region

Image removed due to copyright restrictions. Please see Fig. 2 in Linfoot, E. H., and Wolf. "Phase Distribution Near Focus in an Aberration-Free Diffraction Image." *Proceedings of the Physical Society B* 69 (August 1956): 823-832.

Assumes:
- Small angles (paraxial)
- N large (Debye approximation)

McCutchen

JOSA 54, 240-244 (1964)

3-D pupil

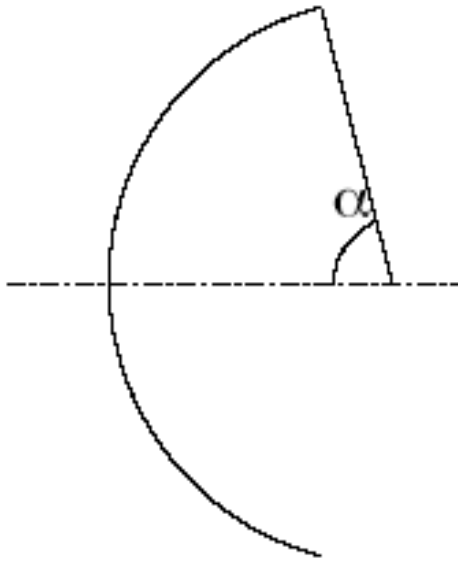

3-D point spread function *h* is 3-D Fourier transform of 3-D pupil (cap of spherical shell, Ewald sphere)

Two cases for Debye approximation

(a)

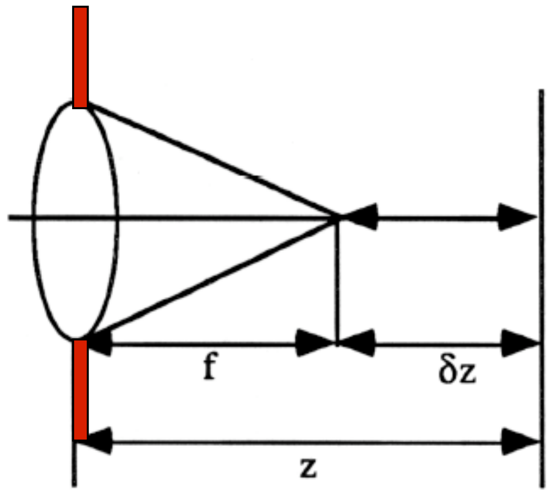

Aperture in plane of lens and N large

$$N = a^2/\lambda z \sim a^2/\lambda f$$

(b)

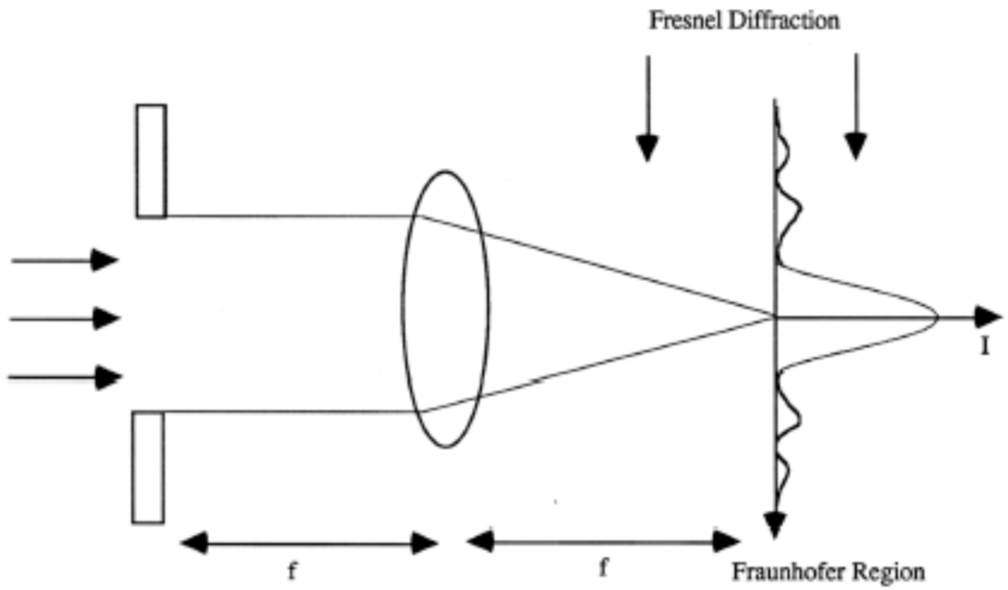

Aperture in front focal plane of lens

Li and Wolf: finite Fresnel number
Debye approximation not valid

$$U_N(P) = B_N(u_N)\exp[i\Phi_N(u_N, v_N)]$$
$$\times \int_0^1 J_0(v_N\rho)\exp(-iU_N\rho^2/2)\rho d\rho,$$

Diffraction of converging wave by an aperture (paraxial theory)

$$u_N = 2\pi N \frac{z/f}{1 + z/f},$$

$$v_N = 2\pi N \frac{r/a}{1 + z/f}.$$

Image removed due to copyright restrictions.
Please see Fig. 4b in Li, Yajun, and Emil Wolf.
"Three-dimensional intensity distribution near the focus in systems of different Fresnel numbers."
Journal of the OSA A 1 (August 1984): 801-808.

$$u_N = \frac{u}{1 + u/2\pi N} \qquad u = \frac{2\pi}{\lambda}\left(\frac{a}{f}\right)^2 z,$$

$$v_N = \frac{v}{1 + u/2\pi N} \qquad v = \frac{2\pi}{\lambda}\left(\frac{a}{f}\right) r,$$

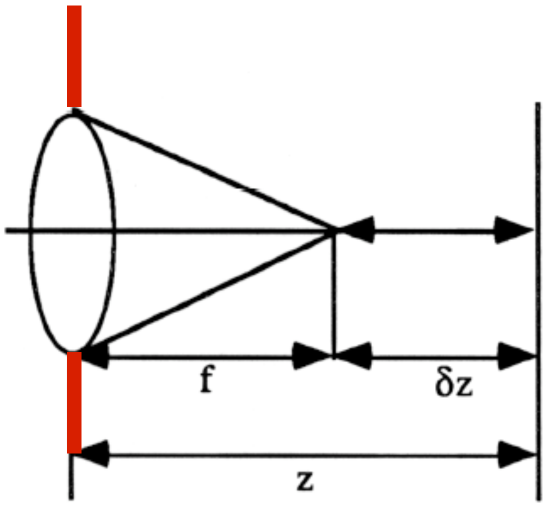

Maximum in intensity no longer at focus - focal shift

Three-dimensional intensity distribution near the focus in systems of different Fresnel numbers

Vol. 1, No. 8/August 1984/J. Opt. Soc. Am. A 801

Tight focusing of light

- Microscopy
- Laser micromachining and microprocessing
- Optical data storage
- Optical lithography
- Laser trapping and cooling
- Physics of light/atom interactions
- Cavity QED

Focusing by high numerical aperture (NA) lens (Debye approximation)

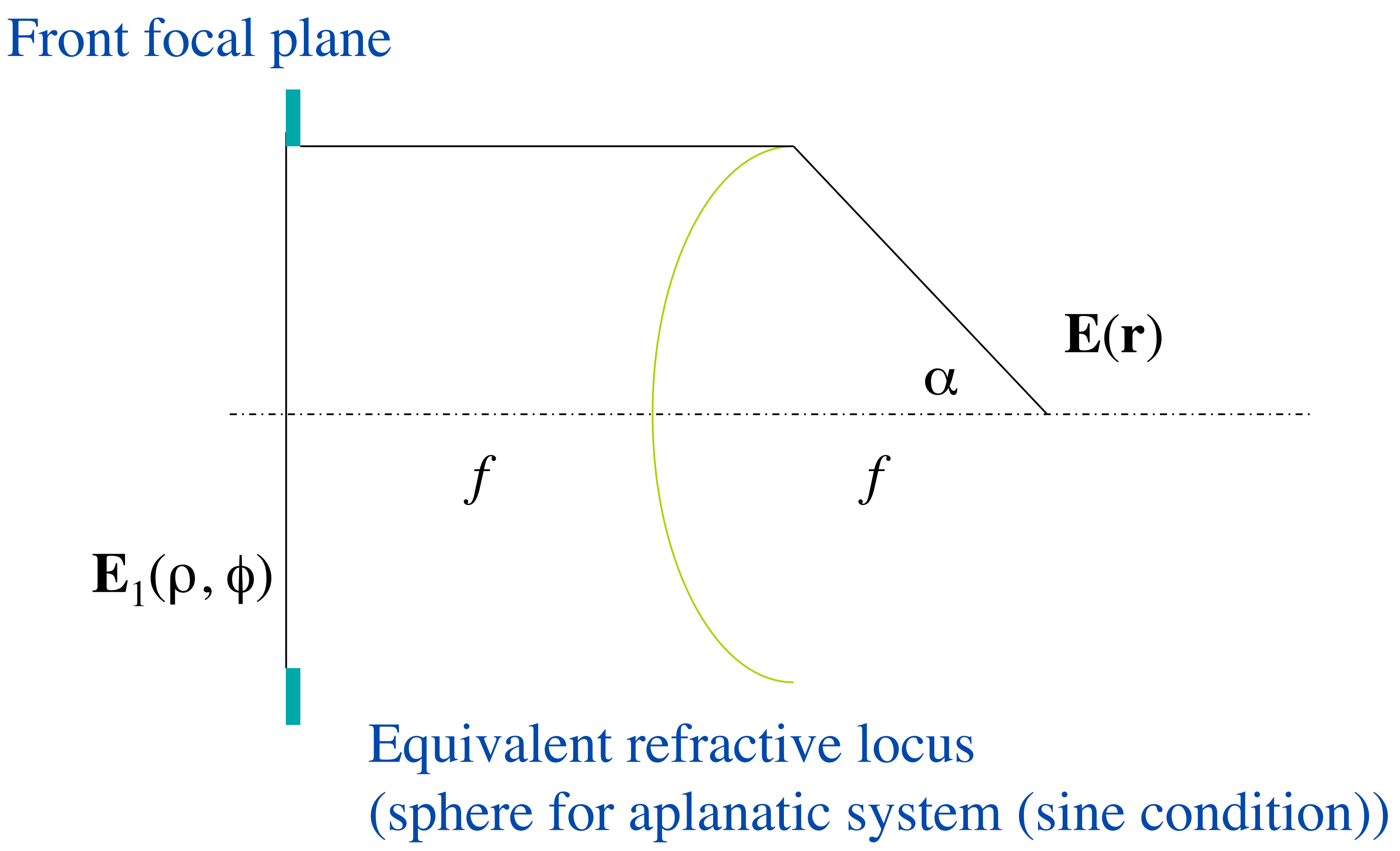

A plane polarized wave after focusing: Polarization on reference sphere

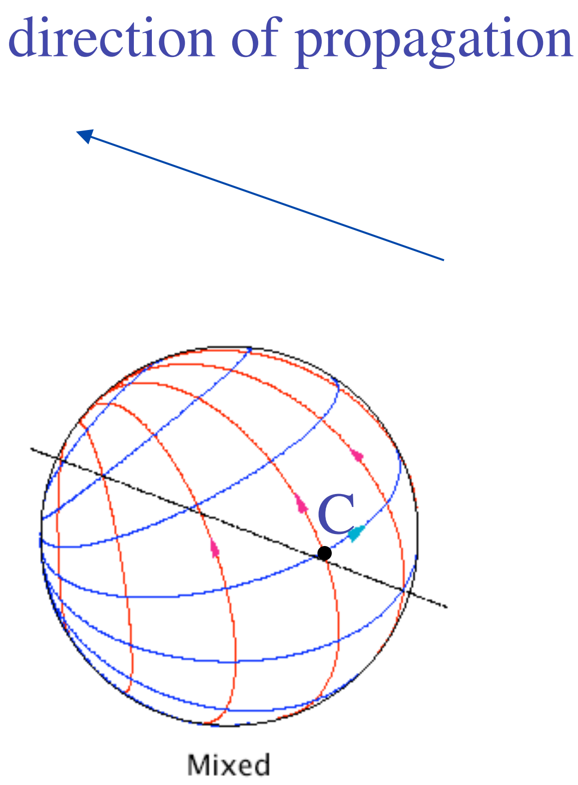

- $\mathbf{p}_x$ (electric dipole along *x* axis)
- $\mathbf{m}_y$ (magnetic dipole along *y* axis)
- C is nearly linear polarization
- Richards & Wolf polarization

Richards and Wolf, 1959

Angular spectrum of plane waves

$$\left.\begin{aligned} e_x(P) &= -\mathrm{i}A(I_0 + I_2\cos 2\phi_P), \\ e_y(P) &= -\mathrm{i}AI_2\sin 2\phi_P, \\ e_z(P) &= -2AI_1\cos\phi_P, \end{aligned}\right\}$$

where

$$\left.\begin{aligned} I_0 = I_0(kr_P, \theta_P, \alpha) &= \int_0^\alpha \cos^{\frac{1}{2}}\theta\sin\theta(1+\cos\theta)\,J_0(kr_P\sin\theta\sin\theta_P)\,\mathrm{e}^{\mathrm{i}kr_P\cos\theta\cos\theta_P}\,\mathrm{d}\theta, \\ I_1 = I_1(kr_P, \theta_P, \alpha) &= \int_0^\alpha \cos^{\frac{1}{2}}\theta\sin^2\theta J_1(kr_P\sin\theta\sin\theta_P)\,\mathrm{e}^{\mathrm{i}kr_P\cos\theta\cos\theta_P}\,\mathrm{d}\theta, \\ I_2 = I_2(kr_P, \theta_P, \alpha) &= \int_0^\alpha \cos^{\frac{1}{2}}\theta\sin\theta(1-\cos\theta)\,J_2(kr_P\sin\theta\sin\theta_P)\,\mathrm{e}^{\mathrm{i}kr_P\cos\theta\cos\theta_P}\,\mathrm{d}\theta. \end{aligned}\right\} \quad (2{\cdot}32)$$

↑

Aplanatic factor

I_2: cross-polarization component
I_1: longitudinally-polarized component

Focal plane for aplanatic

Image removed due to copyright restrictions.
Please see Fig. 5 in Sheppard, C. J. R, A. Choudhury, and J. Gannaway.
"Electromagnetic field near the focus of wide-angular lens and mirror systems."
IEE Journal on Microwaves, Optics, and Acoustics 1 (July 1977): 129-132.

Not circularly symmetric

Electromagnetic field near the focus of wide-angular lens and mirror systems

C.J.R. Sheppard, A. Choudhury and J. Gannaway

MICROWAVES, OPTICS AND ACOUSTICS, JULY 1977, Vol. 1, No. 4 129

Focus of an aplanatic lens

Image removed due to copyright restrictions.
Please see Fig. 6 in Sheppard, C. J. R., and P. Török.
"Efficient calculation of electromagnetic diffraction in optical systems using a multipole expansion."
Journal of Modern Optics 44 (1997): 803-818.

C. J. R. SHEPPARD and P. TÖRÖK

Efficient calculation of electromagnetic diffraction in optical systems using a multipole expansion

JOURNAL OF MODERN OPTICS, 1997, VOL. 44, NO. 4, 803–818

Bessel Beam

Annular mask

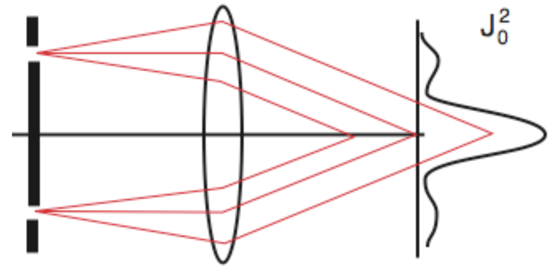

Axicon
(McLeod, 1954)

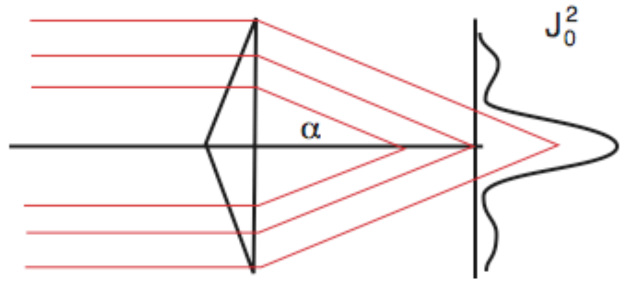

Diffractive axicon
(Dyson, 1958)

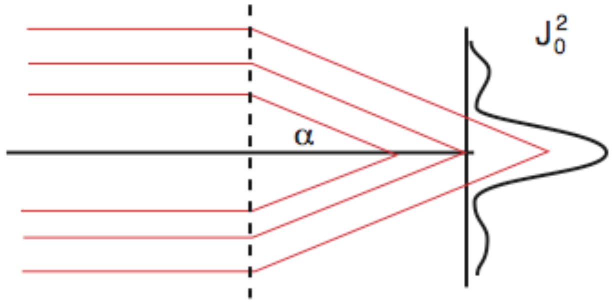

Bessel beam

J_0 beam propagates without spreading:

A wave with zero-order Bessel-function radial distribution propagates without change.

C. J. R. Sheppard and T. Wilson, "Gaussian-beam theory of lenses with annular aperture," IEE J. Microwaves, Opt. Acoust. **2**, 105–112 (1978).

Image removed due to copyright restrictions.
Please see Fig. 2 in Sheppard, C. J. R.
"Electromagnetic field in the focal region of wide-angular annular lens and mirror systems."
IEE Journal of Microwaves, Optics, and Acoustics 2 (September 1978): 163-166.

Time-averaged electric energy density for plane polarized illumination

(e.g. with mirror)

C. J. R. Sheppard, "Electromagnetic field in the focal region of wide-angular annular lens and mirror systems," IEE J. Microwaves, Opt. Acoust. **2**, 163–166 (1978).

Annulus at high NA: circular polarization or TM0 (radial polarization)

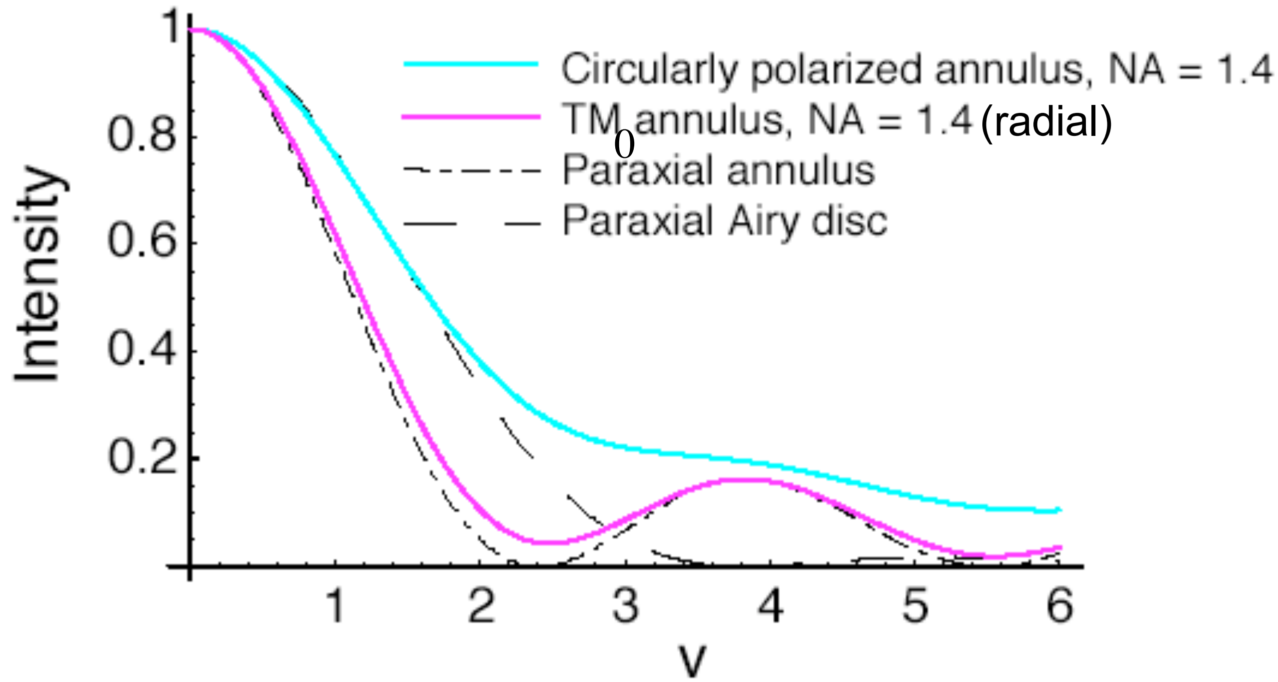

- Paraxial: annulus narrower than Airy
- High NA: circular polarized annulus is ~ same width as Airy
- High NA: TM0 annulus is similar to paraxial

Annular pupils, radial polarization, and superresolution

Colin J. R. Sheppard and Amarjyoti Choudhury

4322 APPLIED OPTICS / Vol. 43, No. 22 / 1 August 2004

Polarization on reference sphere

red: electric field

blue: magnetic field

direction of propagation

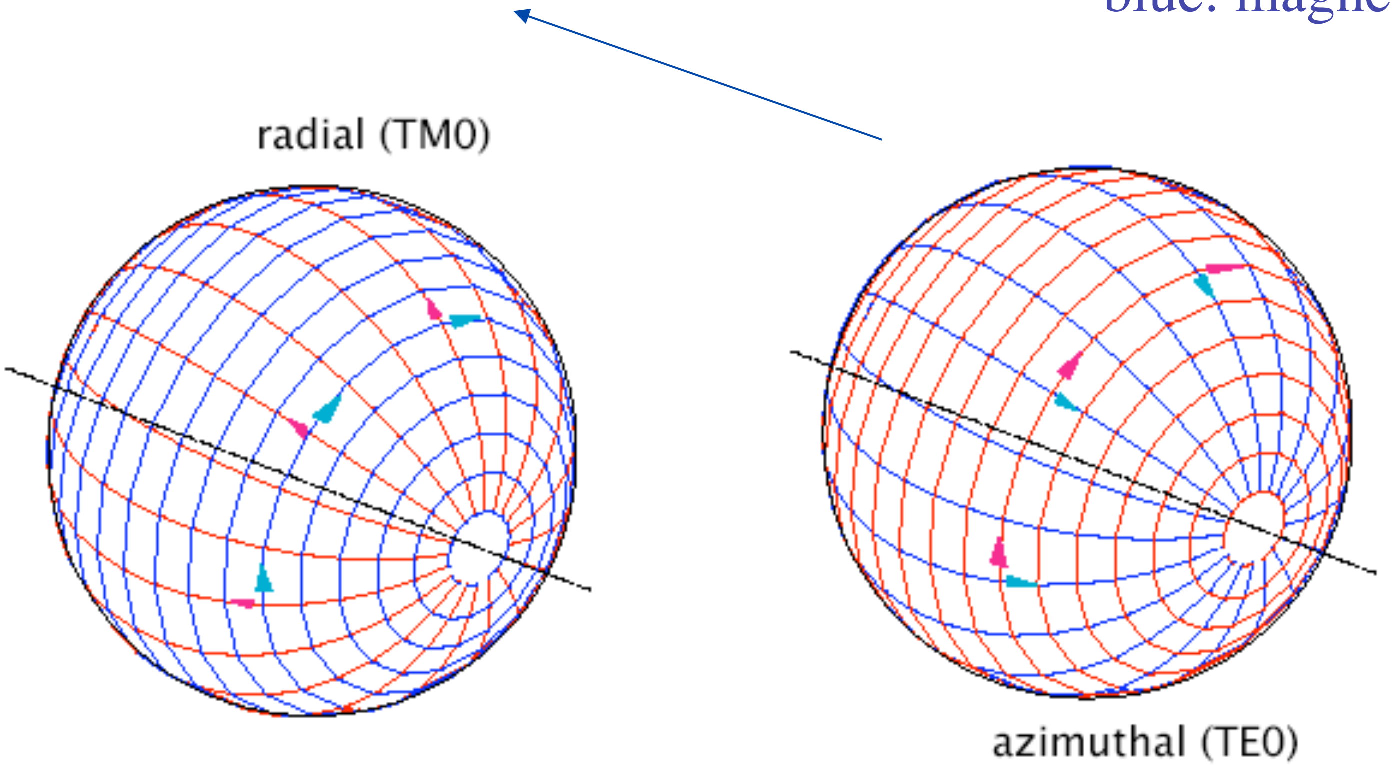

Radial polarization with phase mask

Electric dipole wave:
Ratio of focal intensity to power input

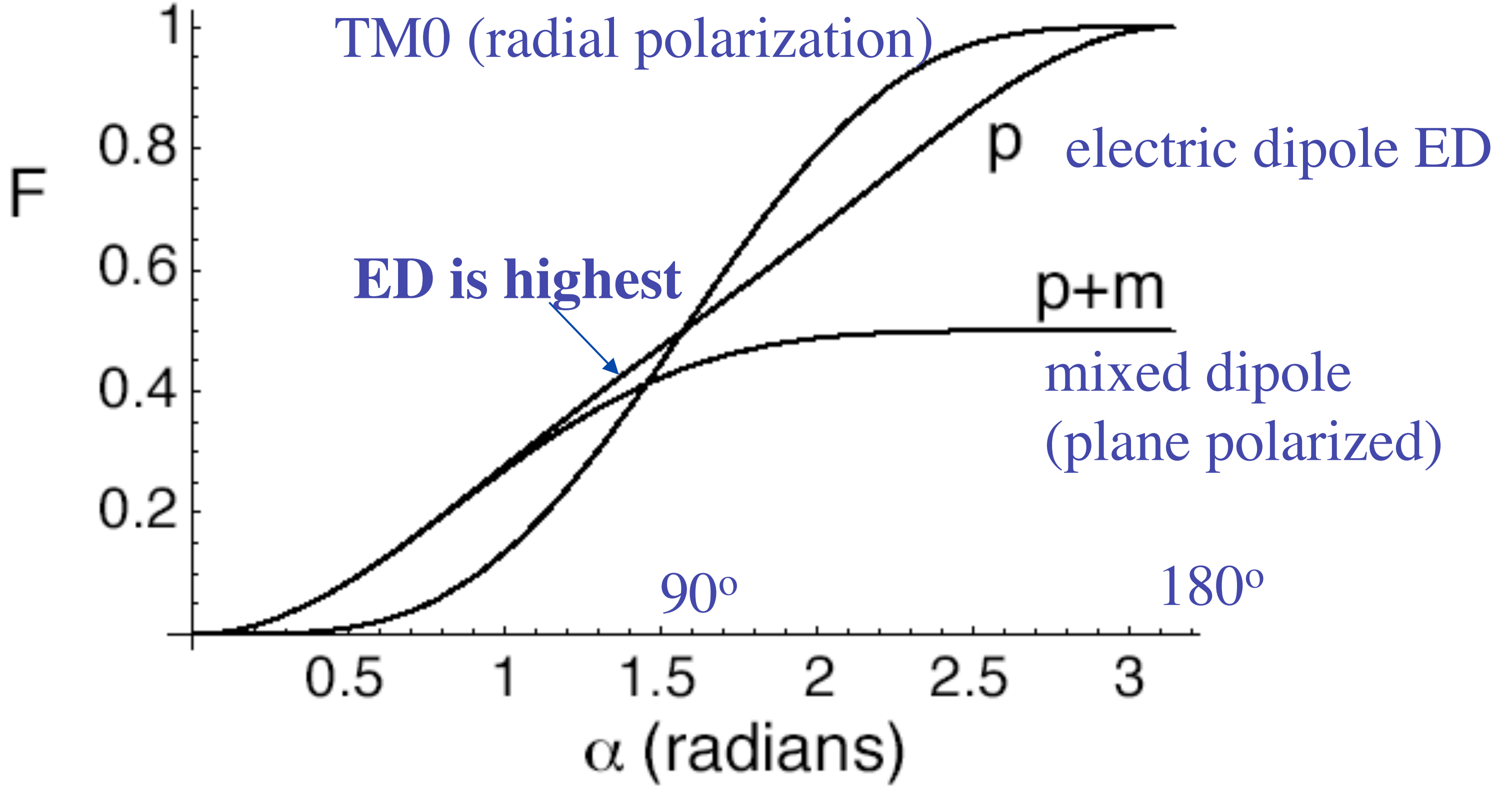

C. J. R. Sheppard and P. Török,
"Electromagnetic field in the focal region of an electric dipole wave,"
Optik **104**, 175-177 (1997).

Polarization of ED on reference sphere

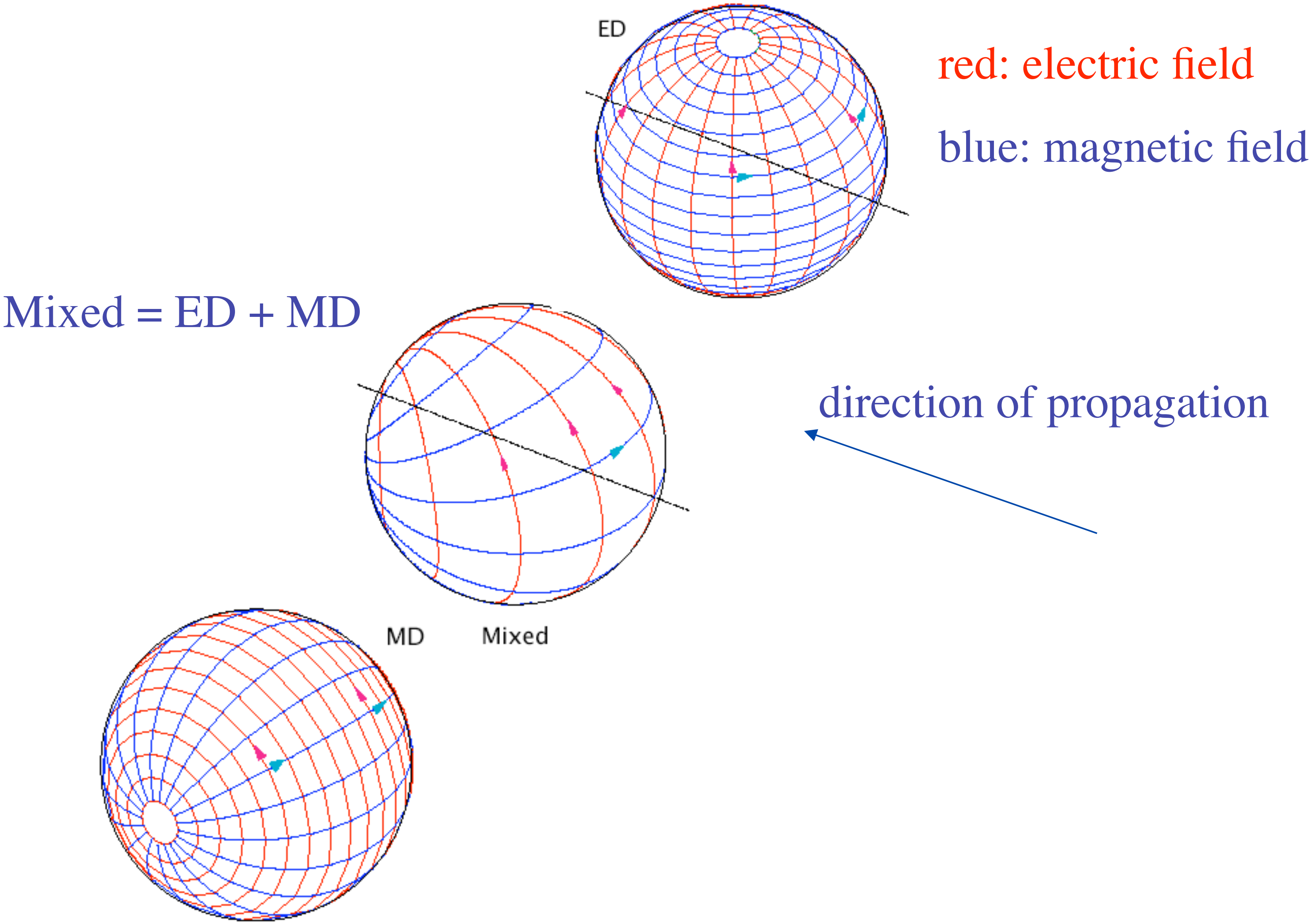

Bessel beams: TE1 polarization

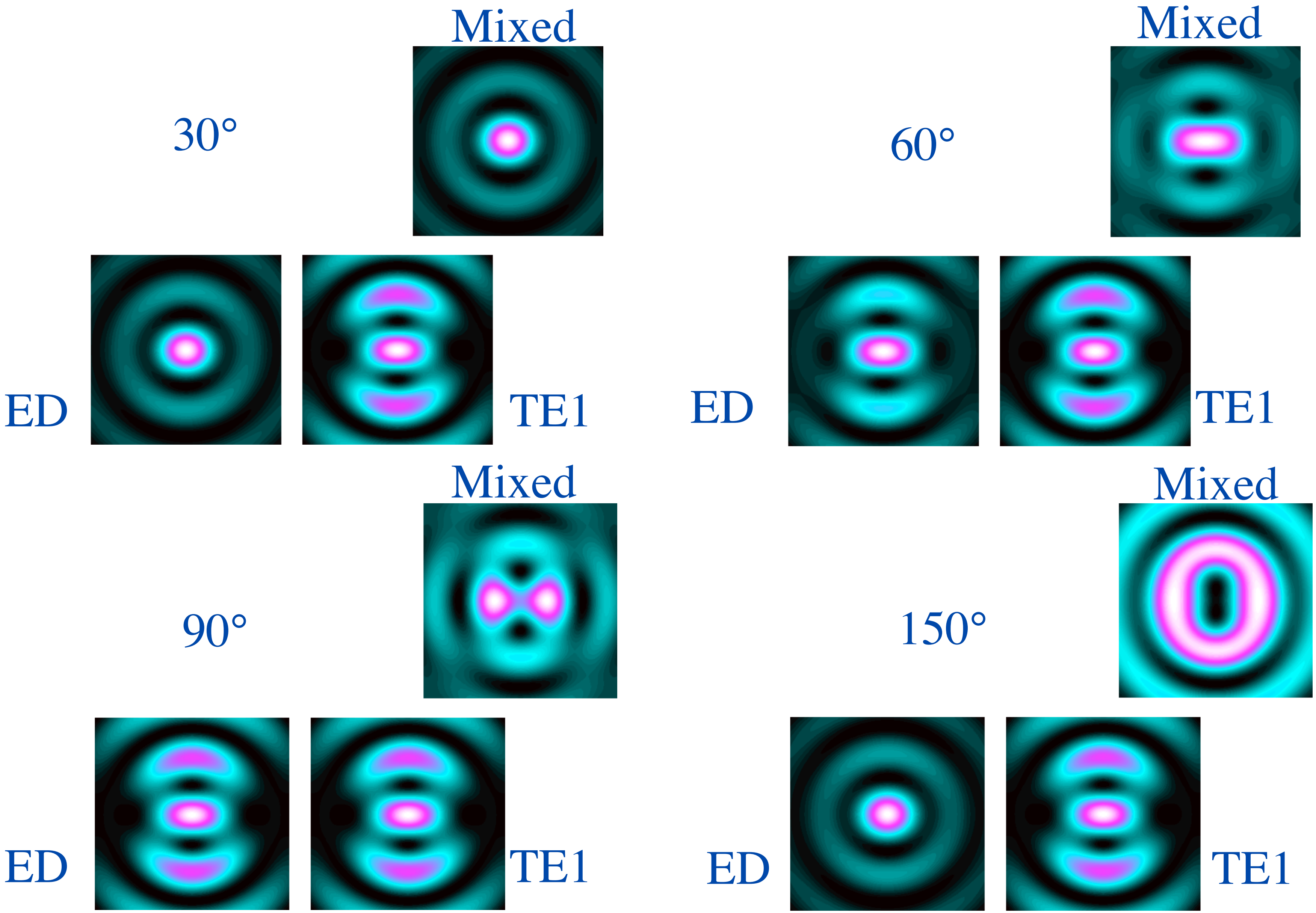

Polarization on reference sphere

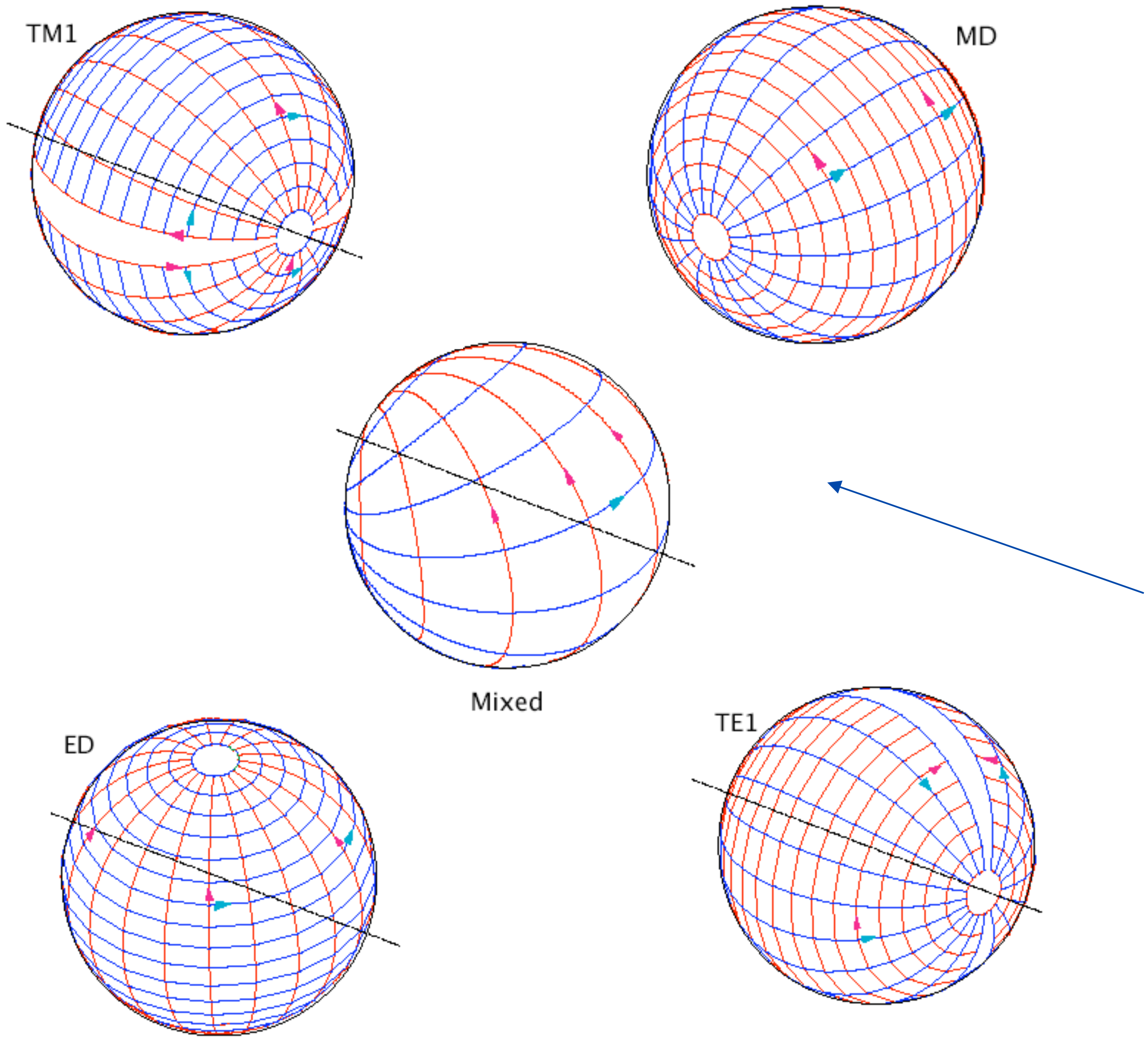

Polarization of input wave

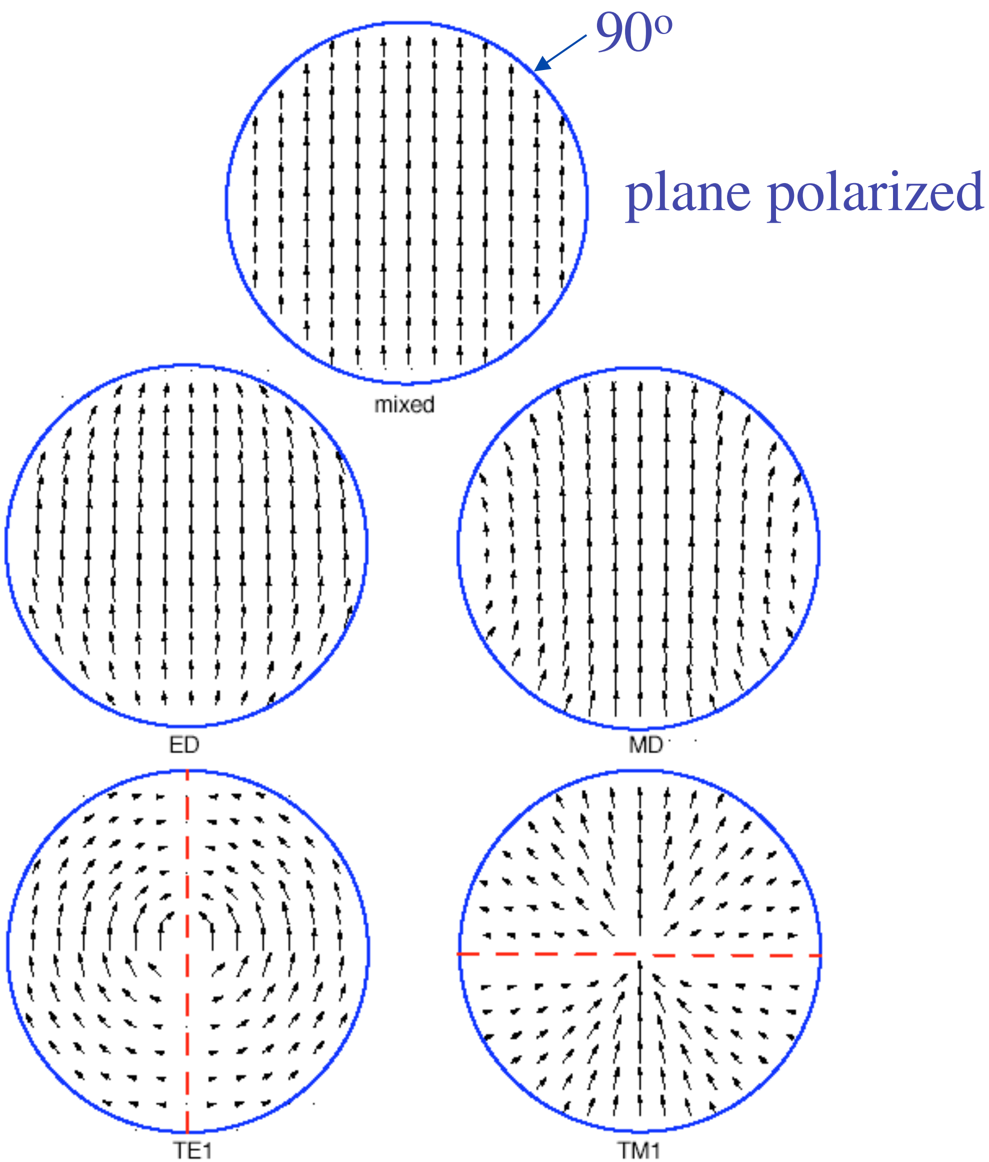

(azimuthally polarized) (radially polarized)

Area of focal spot

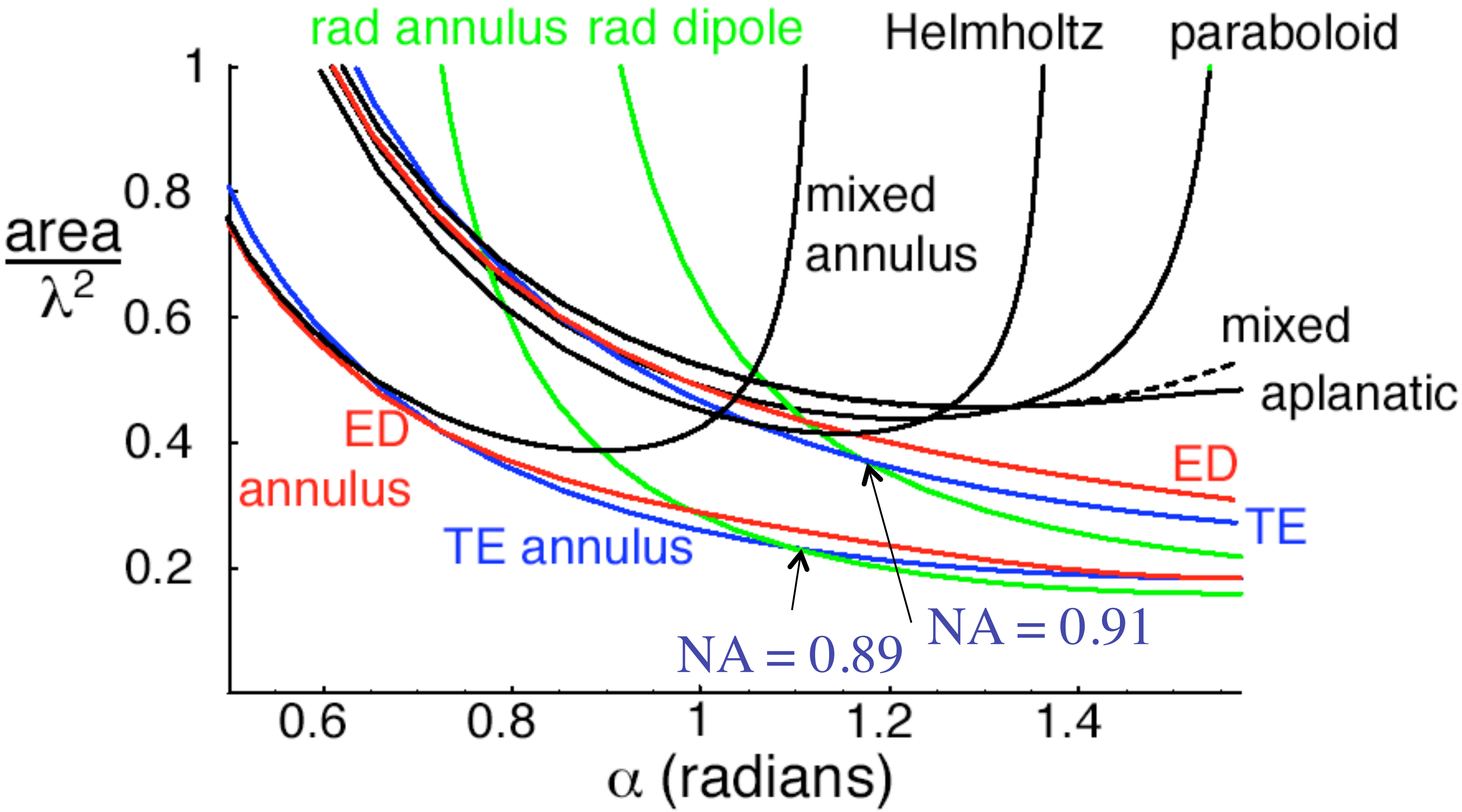

Rotationally symmetric beams

- TM0 = radial polarized input (longitudinal field in focus)
- TE0 = azimuthal polarization

- *x* polarized + *i* *y* polarized = circular polarized
- $TE1_x + i\, TE1_y$ = azimuthal polarization with a phase singularity (bright centre)
- $ED_x + i\, ED_y$ = elliptical polarization with a phase singularity (bright centre)
- ($TM1_x + i\, TM1_y$ = radial polarization with a phase singularity)
- Same G_T as for average over ϕ

Bessel beams: Transverse behaviour for rotationally symmetric (also average over ϕ)

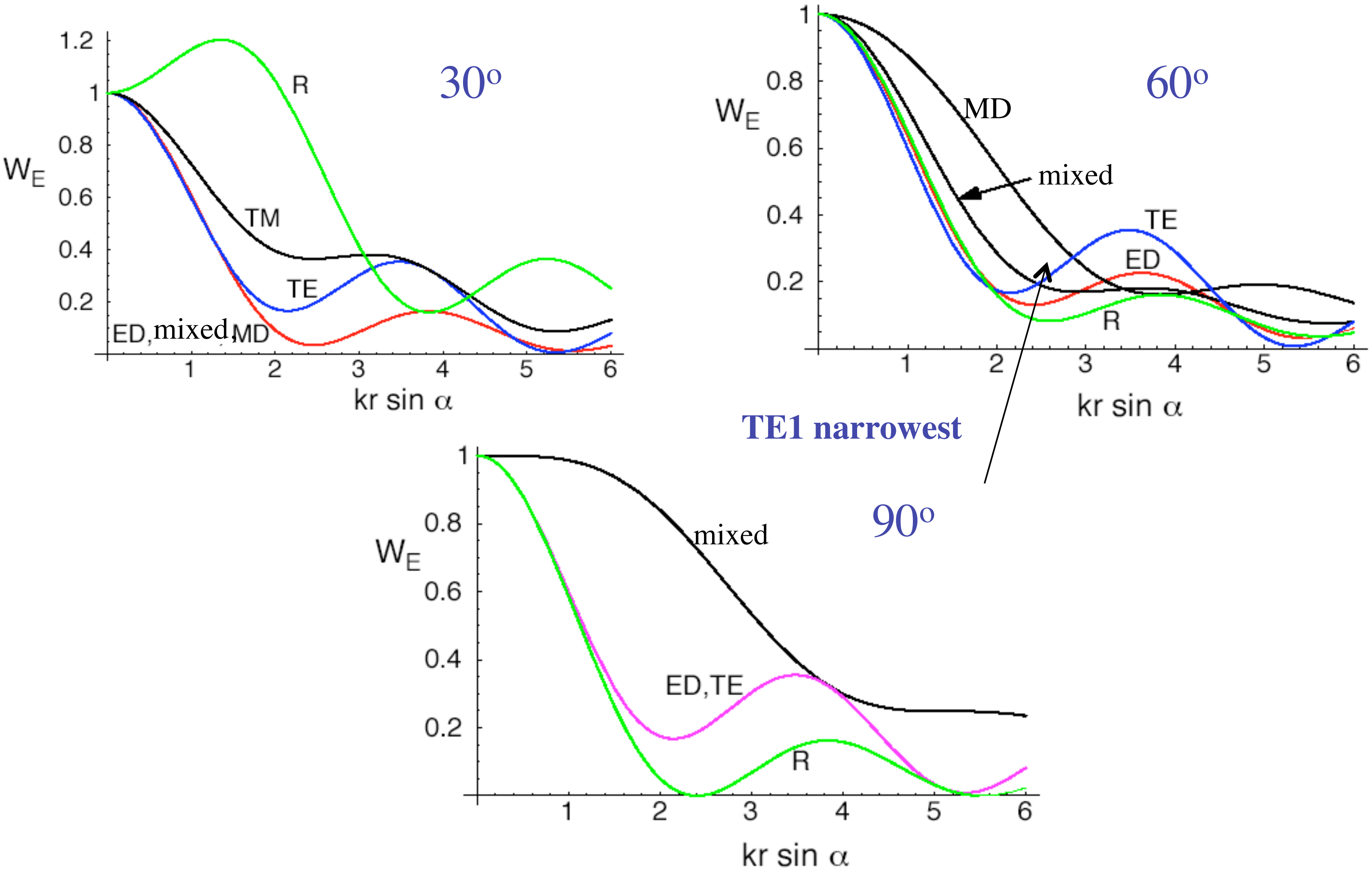

Normalized width for rotationally symmetric

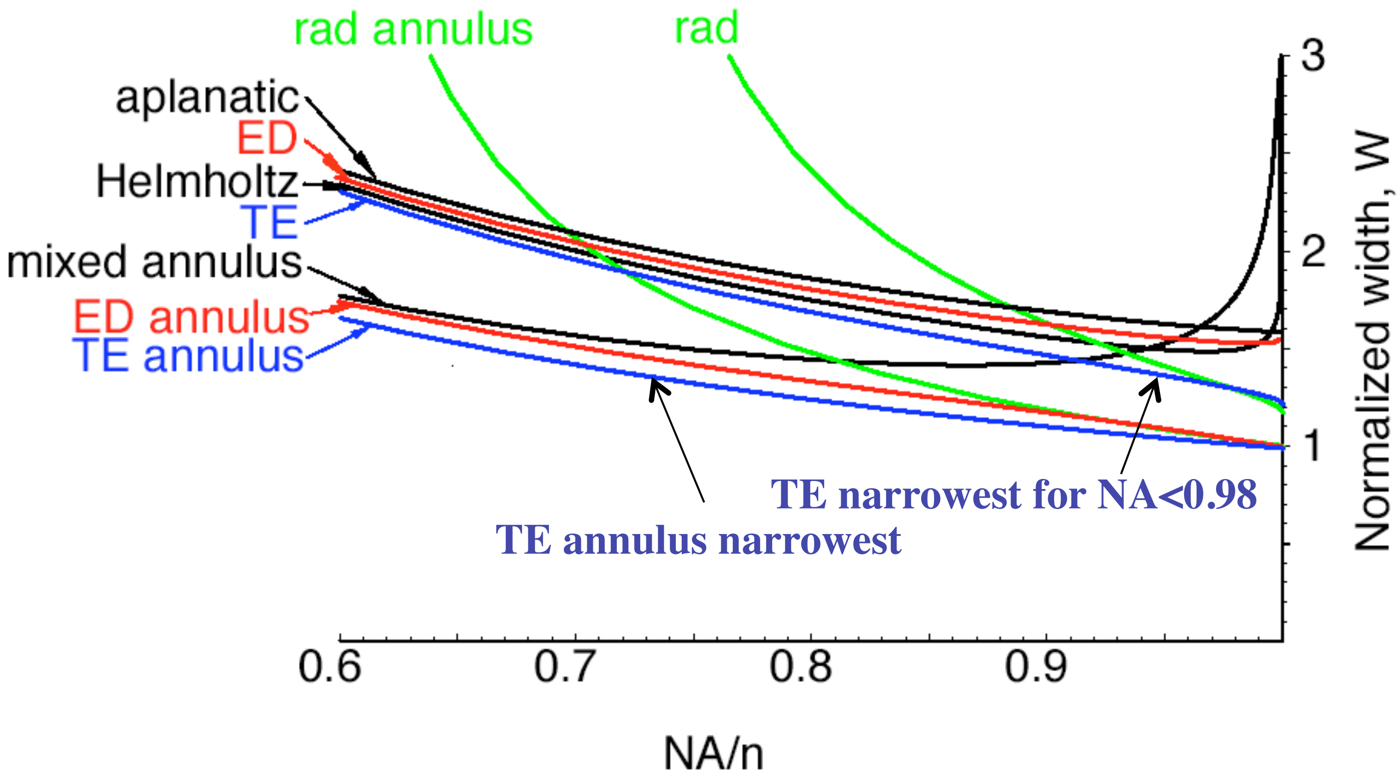

TE = azimuthal polarization with phase singularity (vortex)

Bessel beams for rotationally symmetric

Transverse gain

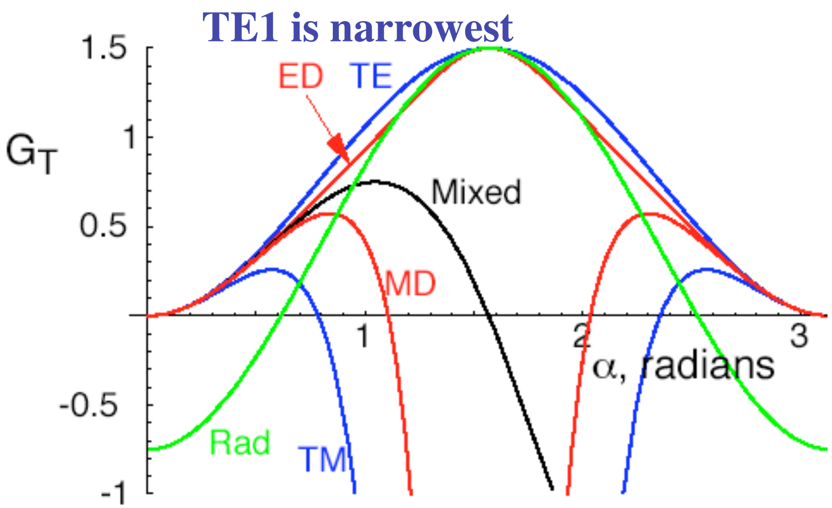

Side lobes

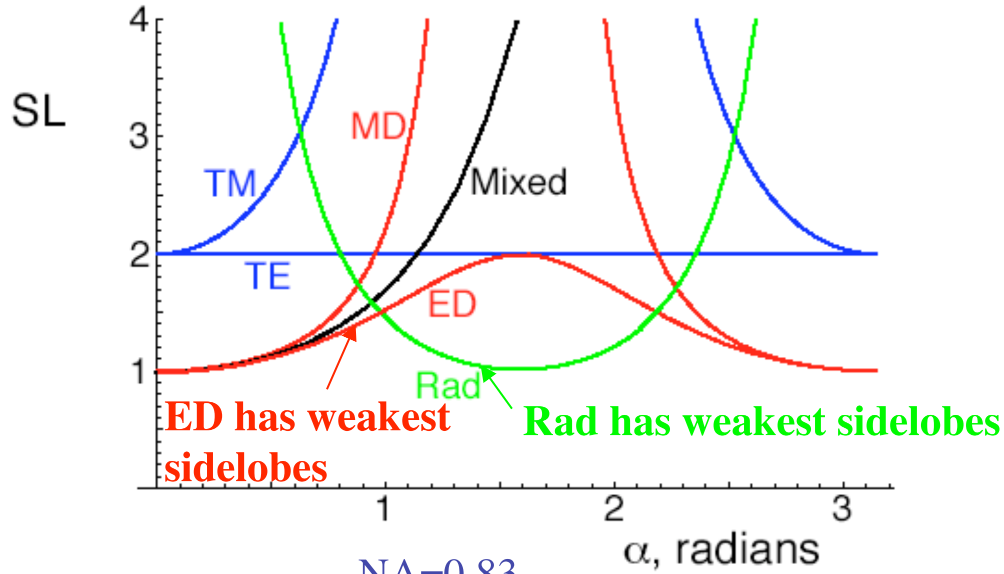

NA=0.83

Eccentricity

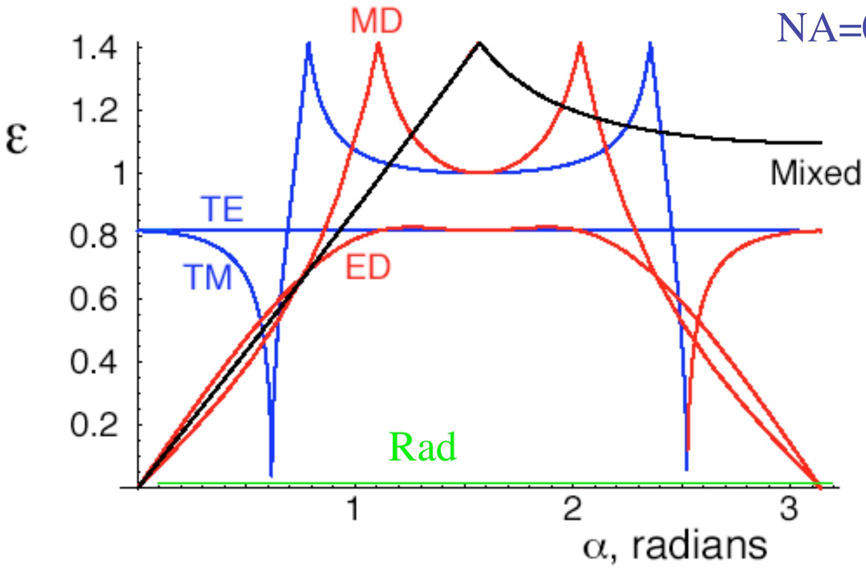

Conclusions

- Focusing plane polarized light results in a wide focal spot
- Focusing improved using radially polarized illumination
- Strong longitudinal field on axis
- Electric dipole polarization gives higher electric energy density at focus
- Transverse electric (TE1) polarization gives smallest central lobe (smaller than radial for Bessel beam)
- TE is asymmetric: symmetric version is azimuthal polarization with a phase singularity (vortex)

2.71 / 2.710 Optics
Spring 2009